The money-inflation nexus revisited

Ringwald, Leopold; Zörner, Thomas

DOI:
10.57938/6bc2dd5b-c206-4062-822b-9b88c247a3b1

Published: 01/01/2021

Document Version:
Publisher's PDF, also known as Version of record

Document License:
Unspecified

Department of Economics
Working Paper No. 310

The money-inflation nexus revisited

Leopold Ringwald
Thomas Zörner

March 2021

WIRTSCHAFTS
UNIVERSITÄT
WIEN VIENNA
UNIVERSITY OF
ECONOMICS
AND BUSINESS

The money-inflation nexus revisited*

LEOPOLD RINGWALD and THOMAS O. ZÖRNER

Vienna University of Economics and Business

Abstract

This paper proposes a Bayesian Logistic Smooth Transition Autoregressive (LSTAR) model with stochastic volatility (SV) to model inflation dynamics in a nonlinear fashion. Inflationary regimes are determined by smoothed money growth which serves as a transition variable that governs the transition between regimes. We apply this approach on quarterly data from the US, the UK and Canada and are able to identify well-known, high inflation periods in the samples. Moreover, our results suggest that the role of money growth is specific to the economy under scrutiny. Finally, we analyse a variety of different model specifications and are able to confirm that adjusted money growth still has leading indicator properties on inflation regimes.

Keywords: Money-inflation link, Nonlinear modeling, Bayesian inference, LSTAR-SV model.

JEL Codes: C11, C32, E31, E51

Acknowledgments

We are indebted to Florian Huber for many insightful comments and suggestions that improved the quality of the paper significantly.

*Address: Department of Economics, Vienna University of Economics and Business. Welthandelsplatz 1, 1020 Vienna, Austria. Corresponding author Thomas Zörner

1 Introduction

The nexus between inflation and money growth is of central interest for economists in general and for policy makers in particular. The importance of this question is reflected in the agendas of almost all central banks in developed economies and tackles the question of how prices can be influenced with a limited set of monetary policy tools. In this article, we provide an updated empirical view on the impact of money aggregates on inflation by explicitly taking the nonlinear relationship between money and price dynamics into account.

In the realm of monetary policy analysis, be it on a theoretical or empirical level, much thought and scientific effort went into the research of the relationship between money and prices. Naturally, since both are in their well established linkage fundamental economic phenomena occurring in modern economies and as such obligatory variables in macroeconomics. This is evidenced by the monetary policy agenda of central banks in steering the latter through controlling the former, mainly via the instrument of setting the key interest rate – or in other words: the opportunity cost of holding money. Ultimately, central banks intend to meet their main objectives, such as maintaining price stability or hitting an inflation target and, either as a direct or indirect aim, maximizing employment as well as counteracting shocks to and supporting economic growth in general.

Given the importance of this relation, it is not surprising that a lot of research effort both went into and is still conducted on this topic. Starting from the well-known quantity theory of money, a discussion of the phrase "inflation is always and everywhere a monetary phenomenon" (Friedman, 1963) evolved. While a detailed review of the relevant literature is not the main scope of this paper, we build on this notion and align to the following streams of literature to empirically revisit the money-inflation nexus in depth. While money growth (specifically the broad aggregate M3 growth) seems to have lost predictive power for price stability since the 1990s (for the US and Euro area alike, see, e.g., Stock and Watson, 2007; Assenmacher-Wesche and Gerlach, 2008; Sargent and Surico, 2011), monetary aggregates may still play an important role for future inflation dynamics. Hence, not only from a central banker's view, a thorough empirical treatment is in order.

Being more specific, our consecutive analysis rests on Amisano and Fagan (2013), who empirically show that despite the weakened predictive power money growth has for inflation in general, it may provide leading indicator information on regime shifts in inflation and, thus, should not be outright dismissed in the conduct of monetary policy. They rest their model choice on two streams of literature. First, a regime switching approach may be appropriate in modeling inflation (see, e.g., Benati, 2008; George and Oxley, 2008; Bordo and Orphanides, 2013), and second, money growth may be indicative of regime switches in inflation while being weakly informative in predicting it directly (see, e.g., Woodford, 1994; Sarno *et al.*, 2003; Brazier *et al.*, 2008; Gürkaynak *et al.*, 2010). Building on these studies, they model inflation as a Bayesian Markov-Switching process where the transition probability of a regime switch depends on a smoothed measure of money growth. In a similar vein, Kaufmann (2015) proposes a K-state switching model with time-varying Markov switching transition distributions accompanied by an efficient Bayesian estimation procedure. This model is applied to an Euro area "two-pillar" Phillips curve with monetary and economic variables. Within this setting, different frequency components of inflation may be triggered by low-frequency variables like M3 growth and the cyclical high-frequency component of the output gap. A main finding was again that long-run prospects of inflation are associated with money growth. Hence, the existence of nonlinearities in the money-price relation has been shown in theoretical and empirical setups alike but still leaves room for improvement in terms of model specification, estimation and general robustness issues.

Thus, following Amisano and Fagan (2013), we revisit the idea of shifting inflation from low to high regimes (and vice versa) triggered by money growth on the basis of another class of nonlinear time-series models. Specifically, our empirical methodology rests on the framework of a two-state Logistic Smooth Transition Autoregressive (LSTAR) model that enables us to distinctively take a regime switching behaviour into account. The switch from a low to a high regime and the smooth transition between them is governed by a continuous first-order logistic function, which is bounded between 0 and 1. Moreover, taking the

notion into account that inflation is a fundamental monetary phenomenon, we construct a money growth indicator, which controls for long-run shifts in trend velocity growth and trend output growth. By using different trend-cycle decompositions, we address the question of robustness in an exhaustive way. A second contribution of this paper is thus to present a fully fledged Bayesian analysis which models the conditional mean as an LSTAR process, including its model order, and the conditional variance as an SV process by combining existing algorithms and procedures in the literature. We are thus able to incorporate uncertainty regarding the model order and delay parameter of the transition signal in a direct and straight forward manner as shown by Lopes and Salazar (2006). Lastly, in order to mitigate the adverse effects heteroscedasticity may have on the parameter estimates, the error variance of the model is allowed to vary over time through a stochastic volatility (SV; Taylor, 1982) process. Simultaneously, this allows us to address concerns about separating time variation in the errors from time variation in the conditional mean (Sims, 2001). The resulting LSTAR-SV model is applied to quarterly data from the US, the UK and Canada starting in 1959Q1, 1963Q1, and 1970Q1 respectively until 2018Q4.

Our model successfully identifies well-known high inflation periods in the samples, largely supporting the findings in Amisano and Fagan (2013) that money growth signals transitory pressure in inflation. Additionally, the findings in our paper produce evidence on the correct delay of this signal, which turns out to be non-universal but rather economy specific. Together with an extensive sensitivity analysis, we provide results for time-varying error variances and different trend-cycle decompositions. Thus, the present paper enriches the information set of policy makers and academics alike with respect to the money-inflation relationship and may lead to the consideration of an additional tool in a central bank's repertoire of assessing inflationary risks.

The rest of this paper is organized as follows. Sec. 2 presents the implemented LSTAR-SV model and briefly discusses its estimation. In Sec. 3 we presents the data and the adjustment procedure for the money growth indicator. While Sec. 4 reports the results, Sec. 5 is dedicated to an extensive robustness examination. Finally, Sec. 6 concludes.

2 Econometric Framework

The idea of shifting inflation from low to high regimes (and vice versa) triggered by money growth rests on the framework of a two-state Logistic Smooth Transition Autoregressive (LSTAR) model. First introduced by Teräsvirta (1994) as an extension to the so-called Threshold Autoregressive (TAR; Tong and Lim, 1980) model, the LSTAR model was subsequently refined, extended and applied with great success in various fields including – but not limited to – finance and economics.[1] In this section, we provide the econometric set-up, its Bayesian stance on estimation with a discussion of the employed priors and the derived posterior. Finally, an overview of the Markov Chain Monte Carlo (MCMC) algorithm is provided.

2.1 The econometric model

We model inflation as a two-state Logistic Smooth Transition Autoregressive (LSTAR) process with lag order $k \in \mathbb{N}$, which may be represented as follows

$$y_t = \boldsymbol{\phi}_1' \boldsymbol{z}_t (1 - F_t) + \boldsymbol{\phi}_2' \boldsymbol{z}_t F_t + \varepsilon_t, \tag{2.1}$$

where y_t denotes inflation measured in time $t = 1, \ldots, T$, the vector $\boldsymbol{z}_t = [1, y_{t-1}, \ldots, y_{t-k}]$ contains a constant and lags of y_t, the coefficient parameters are denoted by $\boldsymbol{\phi}_i = (\phi_{i,0}, \phi_{i,1}, \ldots, \phi_{i,k})$ indicating autoregressive (AR) parameters for the constant and each lag k in regime $i = 1, 2$, while $\varepsilon_t \sim \mathcal{N}\left(0, e^{h_t/2}\omega_t\right)$ is the error term with time-varying log-variance h_t and ω_t being i.i.d. standard normal innovations. Finally, the transition function F_t governs the regime transition and will be discussed below.

[1] See van Dijk *et al.* (2002) and Hansen (2011) for an overview.

As the error term is assumed to be Gaussian with zero mean and a time-varying log-variance, the error variance can be described by a stochastic volatility (SV) model.[2] This alleviates a potential bias in the parameter estimates due to an error misspecification and improve their precision. Following Kastner and Frühwirth-Schnatter (2014), we assume that the log-variance, h_t, evolves according to an AR(1) process

$$h_t = \iota + \rho(h_{t-1} - \iota) + \sigma\eta_t, \qquad \eta_t \overset{\text{i.i.d.}}{\sim} \mathcal{N}(0,1), \tag{2.2}$$

where $\iota \in \mathbb{R}$ denotes the unconditional mean of the log-variance, $\rho \in \mathbb{R}$ the persistence, and $\sigma \in \mathbb{R}^+$ the volatility of the log-variance. Furthermore, this SV specification allows us to separate time variation in the error from the time-varying parameters of the conditional mean (see Sims (2001)'s comment on Cogley and Sargent (2001) resulting into Cogley and Sargent (2005)). However, in Sec. 5 we will compare the results obtained with the SV specification to an LSTAR model with constant error variance in order to assess robustness.

The transition from a low inflation regime, $i = 1$, to a high regime, $i = 2$, and the smooth transition between them is governed by the continuous transition function F_t, which is bounded between 0 and 1. Following this interpretation, y_t is a mixture of two distinct, regime-specific AR-models. In our application, the chosen transition function F_t is a first-order logistic function of the following form,

$$F_t(s_t, d, \gamma, c) = \left[1 + \exp\left\{-\frac{\gamma}{\mathrm{sd}(s_t)}(s_{t-d} - c)\right\}\right]^{-1}, \tag{2.3}$$

where the money growth indicator is the transition variable $s_{t-d} \in \mathbb{R}$ and $d \in \mathbb{N}$ denotes the lag of the transition variable (delay parameter).[3] Finally, $\gamma \in \mathbb{R}^+$ denotes the smoothing parameter which determines the speed of said transition, while $c \in \mathbb{R}$ is the threshold or location parameter where the dynamics of the model revolve around. If $s_{t-d} > c$ the transition from a low to high regime is triggered and vice versa. As γ increases the transition accelerates and the limiting case $\gamma \to \infty$ renders it instantaneous, consequently, F_t approaches the indicator function $\mathbb{I}[s_{t-d} > c]$, which yields 1 if the condition $s_{t-d} > c$ is met and 0 otherwise.[4] Moreover, we normalize the smoothing parameter by dividing γ by the standard deviation of the transition variable s_t, in order to ensure its comparability of magnitude across competing models.

In theory any function – as long as its bounded between zero and unity and includes as inputs the transition variable in some relation to a pivot point such as c – could serve as the transition function and in the literature different transition functions, serving different modeling purposes, are used, e.g. exponential function or second-order logistic function (see van Dijk *et al.*, 2002). However, the first-order logistic function presented above is not only the most popular choice in the literature, but its properties may also model regime switching behavior in inflation, triggered by money growth, out of all commonly applied transition functions most fittingly. For instance, one can imagine that the LSTAR specification models an economy, i.e. the underlying data generating process, in which agents are not homogeneous in their sensitivity to money growth regarding their price setting behaviour. In the framework of the aforementioned theoretical models, for instance, this may be reflected by differences at which point agents shift the basis of their heuristic based inflation forecasts (Brazier *et al.*, 2008), or when agents in buffer stock models assess the gravity of given money supply shocks differently, leading to dissimilar portfolio choices in the economy in response to the same shock. Hypothetically, in such scenarios a plausible situation may emerge where one part of the economy still sets prices according to the low regime and the other already according to the high regime – each exhibiting a distinct sensitivity to money growth – resulting in total inflation as a weighted mixture of both regimes.

[2] While, in principle one could opt for a deterministic (generalized) autoregressive conditional heteroscedasticity (GARCH) specification, like Gerlach and Chen (2008), there is some evidence that the SV model outperforms ARCH type models (see, e.g., Kim *et al.*, 1998).

[3] Note that if the transition variable s_{t-d} is just a lag of the observed time series y_t, the model collapses into a Self-Exciting Threshold Autoregressive (SETAR) model.

[4] Hence, the TAR model is nested in the LSTAR model as a special case.

To provide a compact and efficient notation for the consecutive estimation section, we recast Eq. (2.1) to Eq. (2.3) in matrix form, yielding

$$\begin{aligned} \boldsymbol{y} &= \boldsymbol{Z}\boldsymbol{\phi} + \boldsymbol{\varepsilon} \\ \boldsymbol{\varepsilon} &= e^{\boldsymbol{h}/2} \odot \boldsymbol{\omega} \\ \boldsymbol{h} &= \boldsymbol{V}[\iota, \rho]' + \sigma\boldsymbol{\eta} \end{aligned} \tag{2.4}$$

where $\boldsymbol{Z} = \left(z_t'(1 - F_t), z_t' F_t\right)$ denotes the full data matrix, the coefficient vector is given by $\boldsymbol{\phi} = (\boldsymbol{\phi}_1, \boldsymbol{\phi}_2)$, and the vector of the errors is $\boldsymbol{\varepsilon}$ with dimension $N - max(k, d) \times 1$. Consequently, $\boldsymbol{h}$ is the latent time-varying log-variance vector while $\boldsymbol{V}$ is the variance design matrix with the unconditional mean ι and the persistence ρ. Finally, $\boldsymbol{\sigma}$ denotes the volatility of the log-variance. This notation highlights the fact that, conditional on the implicit parameters of the transition function, the LSTAR model is linear in its other parameters, which proves to be a convenient feature for the estimation.

2.2 Bayesian Setup and Prior Specification

As noted above, to circumvent optimization issues of complicated likelihood functions and problems arising due to the data lacking information about the implicit parameters γ and c, we employ a Bayesian approach for inference. A Bayesian setting is in particular favourable for STAR type models due to the ability to a priori adjust the uncertainty surrounding these notoriously elusive parameters, i.e. introducing information before the data does. This permits Bayesian algorithms to be less vulnerable to lacking information from the data in general. Moreover, extending the work of Vermaak *et al.* (2004) from linear AR models to the realm of nonlinearity, Lopes and Salazar (2006) show how the model order k can be integrated as a parameter to be estimated into a Bayesian approach to the LSTAR model. Although inflation is most commonly assumed to follow AR(1) dynamics remaining a priori oblivious to the correct model order and shifting the burden of decision (mostly) on the data is certainly a desirable feature.

Summarizing, the set of all parameters of interest to be estimated is $\Omega = \{\boldsymbol{\phi}, \delta^2, \gamma, c, d, k, \Lambda; \iota, \rho, \sigma^2\}$, where $\boldsymbol{\phi}$ is the coefficient parameter vector, k the model order, and d, γ, c are the implicit parameters of the transition function. The parameters δ^2 and Λ are hyperparameters of ϕ and k, respectively. The SV model parameters are the level ι and the persistence ρ of log variance as well as the volatility parameter σ^2. In the case of one or more parameters excluded from the full set Ω we denote that with a negative subscript, e.g. $\Omega_{-(k,\boldsymbol{\phi})}$.

As the joint prior distribution $p(\Omega)$ has differing domains of its parameters, which ultimately complicates the analysis of the posterior distribution, we recast it into the following hierarchical structure

$$p(\Omega) = p(\boldsymbol{\phi}|k, \delta^2)p(k|\Lambda)p(\Lambda)p(\delta^2)p(d)p(\gamma)p(c)p(\iota)p(\rho)p(\sigma^2). \tag{2.5}$$

In the derivation above, it has been assumed that the conditional mean parameters $\{\boldsymbol{\phi}, k, \delta^2, \Lambda\}$, the implicit transition function parameters $\{\gamma, c, d\}$ and the conditional variance parameters $\{\iota, \boldsymbol{\rho}, \sigma^2\}$ are each independently distributed. The individual priors in (2.5) are subsequently selected to be, first of all, representative of the respective domain for each parameter as well as flexible regarding their a priori information content and, lastly, chosen in a way to ensure the tractability of the resulting posterior distributions. In general, the prior distributions are set to be conjugate where possible and in most cases specified to contain very little prior information.

Starting with the conditional mean parameter vector $\boldsymbol{\phi}|k, \delta^2 \sim \boldsymbol{\mathcal{N}}_{2(k+1)\times 1}(\boldsymbol{0}, \delta^2\boldsymbol{\Sigma}_{\boldsymbol{\phi}})$, which is a priori assumed to be multivariate normally distributed with each element of the prior mean set to 0 and the diagonal elements of the prior covariance matrix $\boldsymbol{\Sigma}_{\boldsymbol{\phi}}$ set to 10^{10}. Further uncertainty over the latter is introduced via the hyperprior $\delta^2 \sim \mathcal{IG}(\alpha_{\delta^2}, \beta_{\delta^2})$, which follows an Inverse-gamma distribution. The corresponding

hyperparameters are set to $\alpha_{\delta^2} = 2$ and $\alpha_{\delta^2} = 50$. This choice is non-informative and follows the general recommendation in Vermaak *et al.* (2004).[5]

The prior for $p(k|\Lambda) \propto \left[\frac{\Lambda^k}{k!}\right]^{\tau_k} \mathbb{I}_{\mathcal{K}}(k)$ is proportional to a Poisson distribution raised to the power of τ_k and exclusively defined over the support $\mathcal{K}$. $\mathbb{I}_{\mathcal{K}}(k)$ denotes an indicator function that outputs 1 if $k \in \mathcal{K}$ and 0 otherwise. If Λ and τ_k are both less than 1, the prior distribution $p(k|\Lambda)$ is a function of decreasing density as k increases. As τ_k tends to 0 the function approaches a distribution which assigns equal probability to each lag order in $\mathcal{K}$. In our application τ_k is set to 0.5. In order to introduce some variance over Λ, the hyperparameter itself follows $\Lambda \sim \mathcal{G}(\alpha_\Lambda, \beta_\Lambda)$, which is Gamma distributed with shape parameter $\alpha_\Lambda = 2$ and rate parameter $\beta_\Lambda = 0.5$. This specification is chosen to allocate a priori more probability mass on lower and less on higher lag orders as well as to create some uncertainty in the prior distribution for k itself. The set of potential lag orders k, considered a priori here, includes from the mean model with $k = 0$ all lags up to a maximum lag order of $k = 10$, i.e. $\mathcal{K} = \{0, \dots, 10\}$. Since inflation is most commonly modeled as having AR(1) dynamics, this range of potential lag orders should be large enough to sufficiently model its autoregressive properties.

Similarly, the set of the delay parameter d is chosen to contain from an instantaneous money growth signal with $d = 0$ all delay parameters up to a maximum of $d = 16$, i.e. $\mathcal{D} = \{0, \dots, 16\}$, i.e. $p(d) \propto \mathbb{I}_{\mathcal{D}}(d)$ where $\mathbb{I}_{\mathcal{D}}(d)$ denotes an indicator function that outputs 1 if $d \in \mathcal{D}$ and 0 otherwise. It is reasonable to believe that the money signal may take some time to unfold and hence be reflected in inflation. In contrast to Amisano and Fagan (2013), who refrain from estimating the delay parameter inside their model in favor of determining it beforehand based on the cross correlation between inflation and lagged money growth, our approach is more robust since it requires considerably less prior information (or conjecture) about the true delay, as the estimation of and thus the inference on d is purely data-driven.

Regarding the implicit parameters, c and γ, restrictions on their domain must be reflected in their priors as pointed out by Lubrano (2000). Therefore, the prior of the threshold parameter c has to cover at most the range between the minimum and maximum value of the observed transition variables s_t, since the regime switch solely depends on the sign of $s_t - c$. Simultaneously and conveniently, this restriction leads to an economically sensible and direct interpretation of c. Following Gefang and Strachan (2009) the prior of $c \sim \mathcal{U}(a_c, b_c)$ is hence assumed as uniformly distributed between the 95th and 15th percentile of the transition variable, in this way extreme positive and in particular negative outlier values of s_t are eliminated while still forcing little prior information on c. As to γ, the transition function is only defined for positive real numbers by definition and hence only positive values of γ should be considered a priori. However, if $\gamma = 0$ the transition function becomes a constant, i.e. $F_t = 0.5$, hence the nonlinear LSTAR not only collapses into a linear AR model but also becomes unsolveable due to multicollinearity issues. A common choice for the prior of $\gamma \sim \mathcal{G}(\alpha_\gamma, \beta_\gamma)$ is thus a Gamma distribution, which is also applied here.

Up until now all priors were specified to contain very little to almost none prior information. However, in the case of the smoothing parameter some issues arise when specifying its prior too loosely. As noted already by Teräsvirta (1994), a wide range of values for γ will lead to similarly shaped transition functions and hence to little variation in the likelihood function (and thus the posterior distribution). In other words, the data typically contain little information on the smoothing parameter and according to Deschamps (2008) "(...)this reason is commonly invoked to explain the failure of likelihood maximization algorithms in STAR models". On these grounds, the shape and rate parameters of of the γ prior are specified to result in a mean and variance of 10 and 10, i.e. $\alpha_\gamma = 10$ and $\beta_\gamma = 100$. This choice reflects the belief that the signal of money growth does not evolve instantaneously but also depends on the distance between s_t and c. Ultimately,

[5] In principle, the prior for $\boldsymbol{\phi}$ could be chosen to ensure stationarity of the autoregressive process. However, doing so seems undesirable in this application as (i) this paper aims not necessarily on establishing a pure 'forecasting' model and (ii) inflation in the high regime may very well be described by an explosive, i.e. non-stationary, process.

specifying the γ prior loosely or narrowly should have no effect on when, i.e. on the delay parameter d, and at which point, i.e. on the threshold parameter c, the transition occurs.

Lastly, the prior choice of the conditional variance parameters is determined by the R package `'stochvol'` and their specification follows the recommendations in Kastner (2016). The prior Normal distribution of the level parameter $\iota \sim \mathcal{N}(b_\iota, B_\iota)$ is specified with mean $b_\iota = 0$ and variance $B_\iota = 50$, which is fairly vague and designed for data on a percentage scale. The shape parameters of the Beta distribution of the persistence parameter term $(\rho + 1)/2 \sim \mathcal{B}(a_\rho, b_\rho)$ are set to $a_\rho = 5$ and $b_\rho = 1.5$, which translates to a prior mean for ρ of 0.54 with prior standard deviation 0.31. Finally, the a priori Gamma distributed volatility parameter $\sigma^2 \sim \mathcal{G}(\alpha_{\sigma^2}, \beta_{\sigma^2})$ is endowed with shape parameter $\alpha_{\sigma^2} = 0.5$ and rate parameter $\beta_{\sigma^2} = 0.5$, which roughly corresponds to a prior mean of 0 and prior variance of 1, which completes the prior specification.

2.3 Posterior simulation

After discussing the prior distributions, we apply Bayes' theorem and combine the prior with the likelihood function to obtain the posterior distributions. The full posterior distribution is of non-standard form, meaning an analytical solution does not exist and, thus, direct sampling of the full set of parameters is unfeasible. Therefore, a numerical approach in the form of a custom Gibbs sampler (Geman and Geman, 1984) is employed, which in turn requires the conditional posterior distributions for each parameter. While the conditional posteriors of $\boldsymbol{\phi}$, δ^2 and Λ are of standard form, the remaining distributions are not. Therefore, numerical methods embedded in the Gibbs sampler are required to sample from them. As noted before, the coefficient vector $\boldsymbol{\phi}$ is of dimension $2(k+1)\times 1$, hence, as the lag order k changes the dimension of $\boldsymbol{\phi}$ changes as well. It follows that k and $\boldsymbol{\phi}$ have to be sampled jointly, resulting in a non-standard posterior distribution. The Reversible-Jump Markov chain Monte Carlo (RJMCMC; Green, 1995) algorithm is a proven method to account for this change in dimensionality and to search the model space efficiently, as shown for linear AR models by Troughton and Godsill (1998) as well as Vermaak *et al.* (2004) and presented for nonlinear STAR type models by Lopes and Salazar (2006). Regarding the joint distribution of the implicit parameters γ and c, a Multiple-Try-Metropolis (MTM; Liu *et al.*, 2000) algorithm has proven in tests to be slightly more efficient than the standard MH algorithm and thus faster in computation. Lastly, the conditional posterior of d is simply a discrete distribution over $\mathcal{D}$ with posterior probability weights attached to each $d \in \mathcal{D}$ corresponding to their respective likelihood. Sampling from it is relatively straightforward and can be computed directly in a fashion similar but not identical to the Griddy-Gibbs (Ritter and Tanner, 1992) algorithm.

In summary, a Gibbs style sampler is employed to simulate the full posterior distribution of all parameters of interest and the joint conditional posteriors are simulated within an RJMCMC- and MTM-step, respectively.[6] The precise algorithms can be found in Sec. A.1.

3 Data

The choice of countries is chosen based on the availability of sufficiently long data and their relative similarity regarding inflation dynamics. Moreover, the set of economies analyzed by Amisano and Fagan (2013) includes the countries selected here which allows a direct comparison of different regime switching models. Our data set covers the US, the UK and Canada and spans the periods 1959Q1, 1963Q1, and 1970Q1 until 2018Q4, respectively. The dataset for each economy contains the quarterly time series of the price index, a monetary aggregate, as well as the output and is summarized in Tab. 1. With regard to the monetary variables, for each economy the broad money aggregates which are relevant to their respective central banks have been chosen: in particular M2 in the US, M4 in the UK, and M3 in Canada.

[6] The full posterior distribution, $p(\Omega|\boldsymbol{y})$, the conditional posteriors $p(\boldsymbol{\phi}|\boldsymbol{y}, \Omega_{-\boldsymbol{\phi}})$, $p(\delta^2|\boldsymbol{y}, \Omega_{-\delta^2})$, $p(\Lambda|\boldsymbol{y}, \Omega_{-\Lambda})$, and $p(d|\boldsymbol{y}, \Omega_{-d})$ as well as the joint conditional posteriors $p(\gamma, c|\boldsymbol{y}, \Omega_{-(\gamma,c)})$ and $p(k, \boldsymbol{\phi}|\boldsymbol{y}, \Omega_{-(k,\boldsymbol{\phi})})$ can be obtained upon request.

Table 1: Data used in the application.

Economy	Source	Initial date	Terminal date	Money	Inflation	GDP
USA	FRED	1959Q1	2018Q4	M2	CPI	GDP
UK	BoE,ONS,OECD	1963Q1	2018Q4	M4	CPI	GDP
Canada	statcan,OECD,	1970Q1	2018Q4	M3	CPI	GDP

Notes: Federal Reserve Bank of St. Louis (FRED), Bank of England (BoE), U.S. Bureau of Economic Analysis (FRED), Organization of Economic Cooperation and Development (OECD), Office of National Statistics (ONS), Statistics Canada (statcan). For information on the original data sources the reader is referred to Sec. B.1 - Sec. B.3

3.1 Money Growth Indicator

As already noted in Amisano and Fagan (2013), raw money growth may not reveal the full picture of money dynamics due to long-run shifts in trend velocity growth and trend output growth. In that sense, we partly follow their approach and calculate the adjusted money growth indicator, Δm_t^*, by

$$\Delta m_t^* = \Delta m_t + \Delta \tilde{v}_t - \Delta \tilde{y}_t, \tag{3.1}$$

where $\tilde{v}_t$ denotes trend velocity growth and $\tilde{y}_t$ trend output growth.The derivation of this equation can be found in Sec. B.4. As Amisano and Fagan (2013) estimate the trend growth rates of velocity and output by computing one-sided moving averages over several lagged observations, the loss of a non-trivial amount of data points at the beginning of the sample is a clear drawback of this method. For our comparatively shorter sample, this method is deemed too costly, such that we adopt three different techniques to achieve the desired detrending while maintaining as much observations as possible.

We start with another widespread trend-cycle decomposition technique, especially in macroeconomic practice and the real business cycle literature, namely the Hodrick-Prescott (HP; Hodrick and Prescott, 1997) filter. For our application, the one-sided HP filter (see e.g. Stock and Watson, 1999) is chosen to estimate the trend components $\Delta \tilde{v}_t$ and $\Delta \tilde{y}_t$.[7] However, the HP filter is criticised as often as it is applied in practice. The main points of criticism concern (i) the bias of the filtered values at the sample margins (end point bias), (ii) the relative arbitrary ad hoc assumptions regarding the critical tuning parameter λ, and (iii) the generation of spurious cycles as pointed out by Hamilton (2018). As an undisputed, univariate trend-cycle filter does not exist, we alleviate the drawbacks (i) and (ii) to some degree: Firstly, the cause of the end point bias are the strongly changing filter weights at the margins, which lead to excess variability in these periods and, thus, the trend estimate becomes more volatile at the sample end points compared to the middle. Based on spectral analysis Bloechl (2014) proposes a method of flexibly penalizing the filter weights, i.e. the tuning parameter, at the margins to reduce this excess variability. The HP filter used here is augmented in this manner. Secondly, no definitive way exists to calibrate or determine the optimal value for the tuning parameter λ, which is the only explicit choice associated with the application of the HP filter. Ideally, the value for λ should be chosen to reflect prior knowledge about the cycle length. Since the HP filter does not contain an explicit model of the cycle component, λ also directly affects the volatility of the required trend component. In order to select a sensible value for λ it is helpful to analyse the tuning parameter from a frequency-domain perspective (see e.g. King and Rebelo, 1993). Using this approach Maravall and del Río (2007) show that the most commonly applied value for quarterly data, $\lambda = 1600$, corresponds to a cycle length of roughly 10 years. Yet, a cycle horizon of 10 years, which may adequately capture business cycles, does not quite capture the long run behaviour intended in Orphanides and Porter (2001) for the money growth adjustment. Hence, using the

[7] Since the LSTAR model may produce relevant information for policy makers at the margins of the sample, the standard two-sided HP filter which takes past and future data points simultaneously into account to obtain the trend estimate for each point in time t, seems undesirable here.

values provided by Maravall and del Río (2007) λ is set to 10000, which corresponds to a cycle length of approximately 20 years.

Finally, after adjusting raw money growth for trends in output and velocity growth, the resulting money growth indicator is further treated with a moving average MA(q) of the last $q = 5$ observations in order to smooth out temporary shocks with no implication for inflation. Regarding the construction of the rates of change, two natural candidates present themselves in the form of (i) annual rates of change (YoY), and (ii) (annualized) quarterly rates of change (QoQ) since the data used is in quarterly aggregates. While the former is used in Amisano and Fagan (2013), both are actually commonly applied in forecasting various macroeconomic variables such as inflation (see e.g. Stock and Watson, 2006; Faust and Wright, 2013). In principle, the discrepancy between these two rates of change is minor as the annual growth rate is formally equivalent to the average of four annualized quarterly growth rates – essentially a moving average. Yet, conceptually they are different enough to warrant their treatment as separates and since no real formal guidance exists on which measure to prefer in the context of inflation, the model is simply run over both rate of change measures separately.[8] Subsequently, the estimation results are presented on the basis of annual rates of change while results associated annualized quarterly rates of change can be found in the appendix. Moreover, this also implies that the data entering the model (and the adjustment procedure for that matter) are log difference rates of change on a percentage scale, consequently the results have to be viewed and evaluated accordingly.[9]

3.2 Discussion

For each country Fig. 1 to Fig. 3 report on the left side panels the trend growth rates of velocity and output, based on one-sided augmented HP filter estimates. Their effect on raw money growth can be explored on the right hand side where the implied adjusted money growth indicator is plotted against unadjusted money growth (MA(5) smoothed) as well as inflation. Top and bottom panels then divide each of these plots into the respective growth rate measures.

In general across all countries under scrutiny the trend growth rates of output and velocity exhibit an almost similar pattern between the annual and quarterly growth rate measure, which does not necessarily surprise since the trend component is intended to track long-run persistent movements by filtering cyclical noise and annual growth rates basically smooth out some noise of annualized quarterly growth rates. Yet, it also indicates the desired performance of the one-sided augmented HP filter in extracting long-run trends, i.e. not excessively susceptible to deviations in the noisiness of the cyclical component. Consequently, this pattern also translates to both adjusted money growth indicators for each country. Moreover, the movement of long run output and velocity growth appears to generally evolve inversely to each other, as rising trend output growth coincides with decreasing velocity growth (and vice versa) over several, distinct periods of time – which is in so far surprising as output appears in the numerator of velocity. By the nature of the adjustment procedure employed, one would expect that these periods imply marked differences between adjusted and unadjusted money growth. And indeed that is evidently the case.

Taking a closer look on the US, neglecting the adjustment of money growth would have overstated the risk to price stability in the 1960s, at the end of the 1980s, as well as in the period from the late 1990s up to the sample end in 2018Q4 (right hand side panels in Fig. 1). The difference between the adjusted and unadjusted money growth indicator is by definition due to changes in the long-run growth of velocity and output and

[8] In particular, the rate of change formula applied is $\Delta^h x_t = 100 * (4/h) * log(X_t/X_{t-h})$, where $h = 4$ implies the annual rate of change (YoY) and $h = 1$ the annualized quarterly rate of change (QoQ). Note that $\Delta^4 x_t = 100 * log(X_t/X_{t-4}) = 100 * \sum_{i=0}^{3} log(X_{(t-i)}/X_{t-(i+1)}) = \frac{\sum_{i=0}^{3} \Delta^1 x_{(t-i)}}{4}$.

[9] While seasonal patterns are of no concern for annual growth rate calculations, they pose a problem in the annualized quarterly rate of change measure. Therefore seasonally adjusted data were obtained either directly from the source – where possible – or by using X-13ARIMA-SEATS.

in the case of the US it is largely driven by the trend component of velocity growth, as the periods of low to negative trend velocity growth coincide with the aforementioned periods of unadjusted money growth overstating risk to price stability, while output growth does not exhibit such drastic changes in its long run trend (left hand side panels in Fig. 1).

Figure 1: US data.

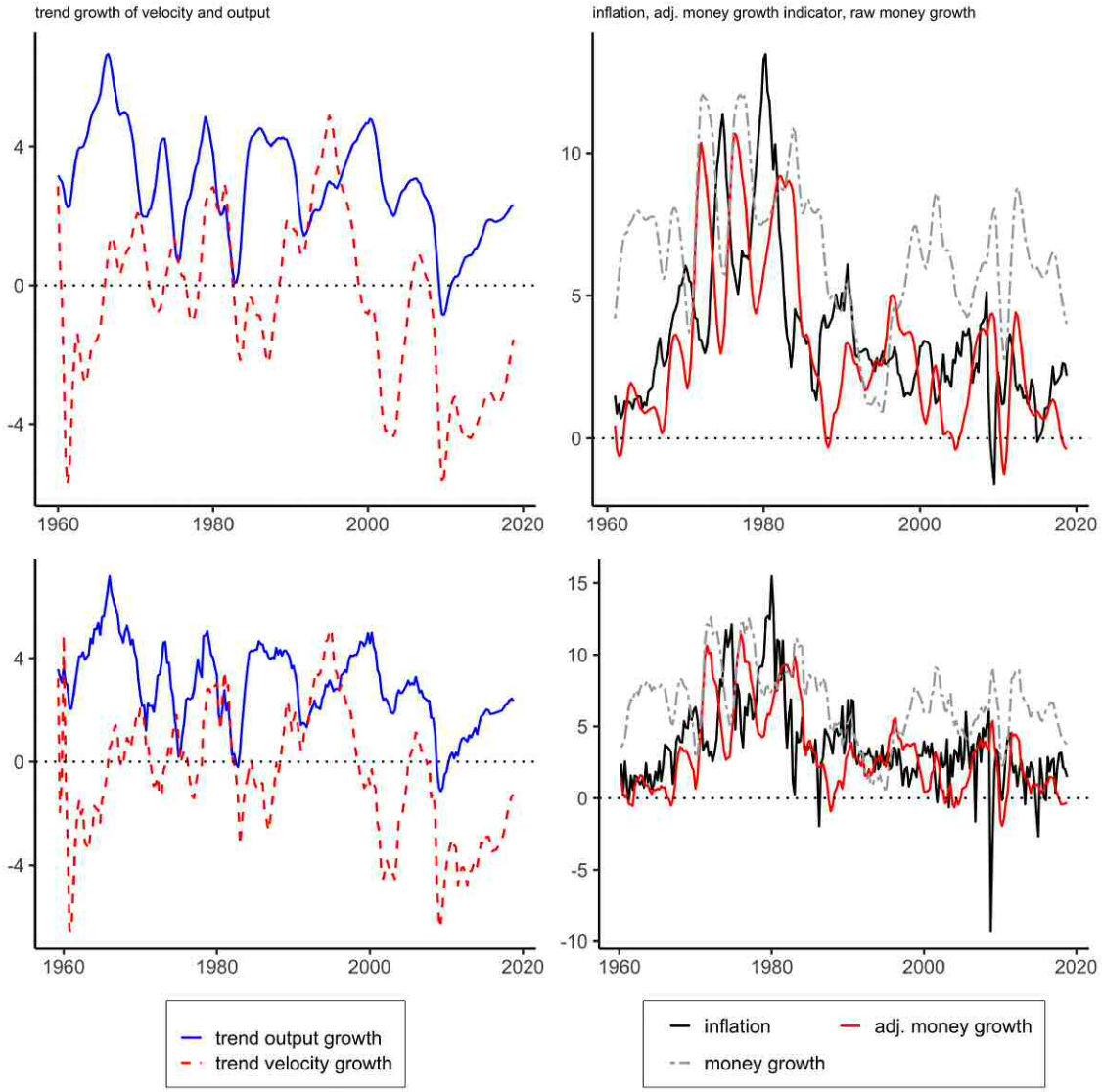

Top panels: annual growth rates (YoY). Bottom panels: annualized quarterly growth rates (QoQ). Left side: trend estimates of output and velocity growth (one-sided augmented HP(10000) filter. Right side: inflation, implied adjusted money growth indicator and MA(5) smoothed raw money growth.

For the UK, Fig. 2 paints a very similar picture. In particular, unadjusted money growth would have overrated pressure on inflation from the mid 1980s to the mid 1990s and again from the early 2000s until the Great Recession. However, it should also be mentioned that the adjusted money growth indicator evidently leads to a moderate understatement of the risk of inflation transitioning to a high regime in the period from the mid to late 1970s compared to unadjusted money growth (right hand side in Fig. 2). However, the estimation

results in the subsequent section show that this understatement is mild enough to nevertheless assign the ensuing global peak of UK inflation to the high regime.

Figure 2: UK data.

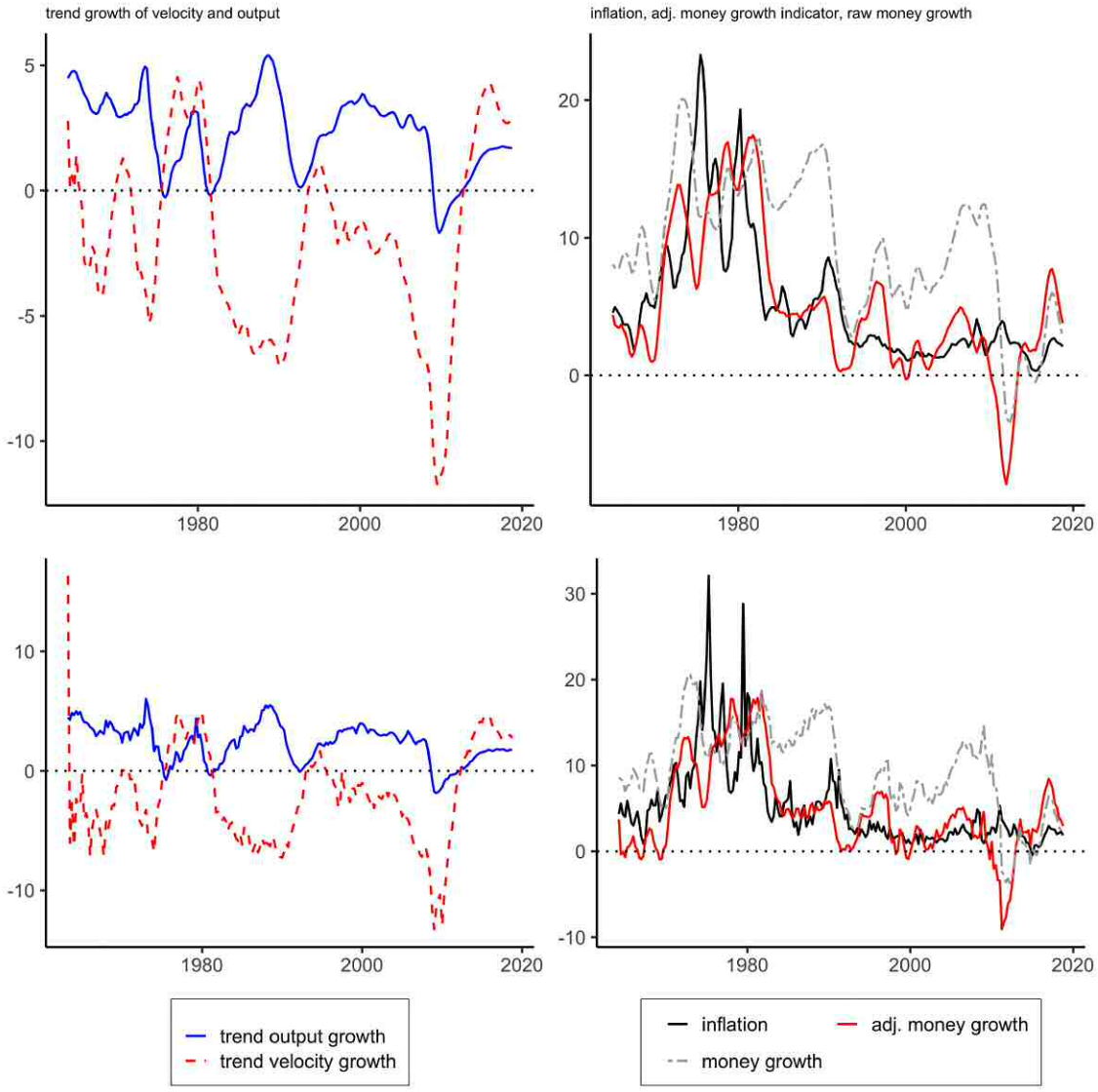

Top panels: annual growth rates (YoY). Bottom panels: annualized quarterly growth rates (QoQ). Left side: trend estimates of output and velocity growth (one-sided augmented HP(10000) filter. Right side: inflation, implied adjusted money growth indicator and MA(5) smoothed raw money growth.

In contrast to the US and UK, the inverse relationship between trend velocity and output growth is hardly the case in Canada as becomes apparent when examining the right hand side panels of Fig. 3. Interestingly enough, quite the opposite can be observed. From the 1980s upwards Canadian trend growth of velocity and output show similar dynamics, almost tracking each other albeit on different levels. Yet, the movements of velocity growth are, again, much more pronounced, leading to marked differences between adjusted and unadjusted money growth over many periods. In particular, the latter may have overstated inflationary pressure from money growth in the years leading to the dip of the Great Recession. However, the adjustment procedure applied may dampen the informational content money has on inflation in the period from the late

1970s to the early 1980s, as the difference between the adjusted and unadjusted money growth indicator is quite large in a rather high inflation period.

Figure 3: Canada data.

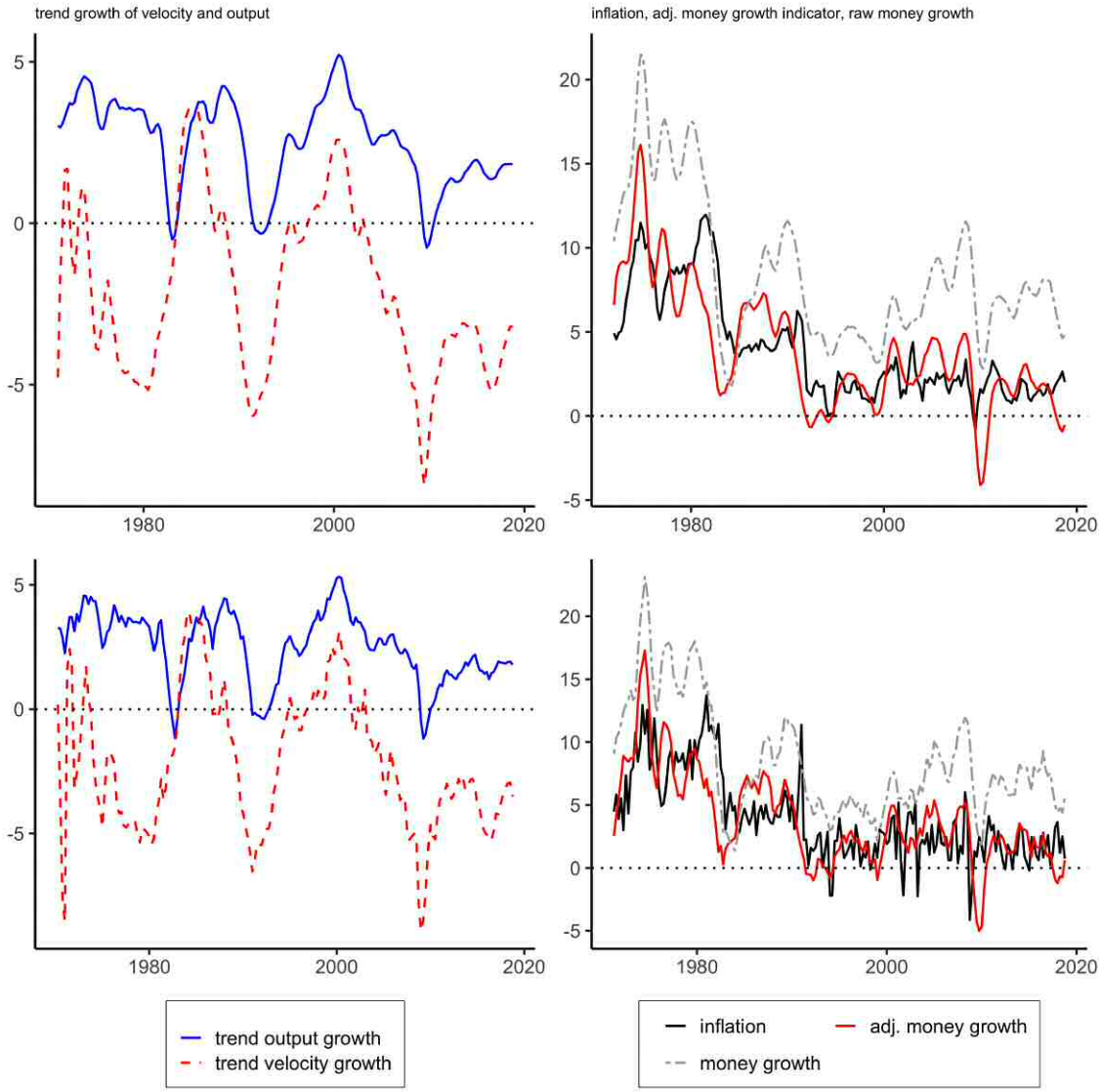

Top panel: annual growth rates (YoY). Bottom panel: annualized quarterly growth rates (QoQ). Left side: trend estimates of output and velocity growth (one-sided augmented HP(10000) filter. Right side: inflation, implied adjusted money growth indicator and MA(5) smoothed raw money growth.

Although the one-sided HP filter estimates trend components of output and velocity growth that appear to lead to plausible adjustments of raw money growth, some uncertainty remains in the choice of this particular filter. Therefore the adjustment procedure is also undertaken on the basis of different filtering techniques for velocity and output growth. In particular, the chosen set of filters includes the already mentioned two-sided HP filter, the rolling window filter employed by Amisano and Fagan (2013), and the regression type filter proposed by Hamilton (2018), which are then compared to the estimates from the one-sided HP filter.[10]

[10]The two-sided HP filter is augmented in a similar fashion as the one-sided variation to alleviate the end point bias. The rolling window filter considers the last 40 observations as in Amisano and Fagan (2013). The parameter h in Hamilton's regression type

Detailed results for annual (YoY) and quarterly (QoQ) rates can be found in Sec. B.5. In order to test the robustness of the main results with regards to the filter type, the LSTAR-SV model is also estimated with money growth indicators based on this selection of alternative filtering techniques in Sec. 5.

4 The role of money growth for inflation

In this section, we present results based on the YoY specification (annual rates of change) in depth and report a brief comparison to the QoQ (annualized quarterly rates of change) results. Detailed results (tables and figures) for the QoQ specification can be found in Sec. C.1. Furthermore, all results are based on the exact same prior specifications (as discussed in Sec. 2.2). The Gibbs sampling scheme is applied to compute 25000 iterations where the first 5000 iterations are discarded as burn-in and the results presented below are computed from the remaining 20000 draws.[11]

Tab. 2 reports the median, 2.5%- and 97.5%-percentiles of the posterior distributions for each of the parameters being estimated, conditional on the most commonly drawn lag order k and delay parameter d. For each country, the results reported below are based on annual rates of change measures, raw money growth adjusted for output, and velocity trends obtained from the augmented one-sided HP filter. The effective sample starts are then 1961Q1 for the US, 1965Q1 for the UK, and 1972Q1 for Canada.

Figures 4-6 include density plots of the parameters of most interest, i.e. c, γ and the regime dependent AR parameters (as well as histograms of k and d), conditional (continuous line) and unconditional (dashed line) on the most visited model order and delay parameter. In this way, the information in the tables is condensed to the most likely combination of model order and delay parameter while the figures provide a sense for the robustness of these results with regards to k and d. It should be noted, however, that in most cases the differences between the conditional and unconditional presentation are negligible. Moreover, the bottom panel of the figures shows the implied and rescaled transition function (calculated at the median of the posterior distribution and based on the most commonly selected k and d) plotted against actual and model fitted inflation. The shaded area under the rescaled transition function indicates the periods, which the model assigns to the high regime or its transitory phases. In addition, the regime specific means of inflation are being reported in the text.[12]

filter is set to $h = 20$ to extract longer cycles than the usual business cycle in order to estimate long run trends comparable to the specification of the other filters. For further information, the reader is kindly referred to the respective, cited literature.

[11] After thorough testing, 25000 iterations were deemed enough for convergence. Moreover, starting values are set according to Livingston and Nur (2017) and convergence was also verified for different starting values. Convergence statistics and plots can be obtained from the authors upon request.

[12] These can be obtained from $\mu_i = \frac{\phi_{i,0}}{1-\phi_{i,1}-\cdots-\phi_{i,k}}, i = 1, 2$, and are computed at the median values of the parameter draws. Conceptually, these are the means of the state distribution around which the dynamics of the series tend to oscillate in each regime. Obviously, the equation above is only defined if the estimated AR process is stationary, which is not necessarily the case as stationarity is not enforced a priori in this application.

Table 2: Posterior estimates, all countries, annual rates of change (YoY).

	Annual rates of change								
	US			UK			Canada		
Parameter	$\theta_{0.5}$	$\theta_{0.025}$	$\theta_{0.975}$	$\theta_{0.5}$	$\theta_{0.025}$	$\theta_{0.975}$	$\theta_{0.5}$	$\theta_{0.025}$	$\theta_{0.975}$
$\phi_{1,0}$	0.26	0.14	0.40	0.08	0.00	0.16	0.52	0.23	1.30
$\phi_{1,1}$	0.91	0.87	0.95	1.56	1.40	1.69	0.71	0.30	0.84
$\phi_{1,2}$	–	–	–	-0.60	-0.73	-0.44	–	–	–
$\phi_{2,0}$	-0.58	-1.25	0.21	2.36	-0.35	6.45	0.01	-0.23	0.30
$\phi_{2,1}$	1.15	1.05	1.24	0.92	0.00	1.63	1.01	0.96	1.05
$\phi_{2,2}$	–	–	–	-0.20	-0.78	0.52	–	–	–
k	1 (100%)	–	–	2 (99.77%)	–	–	1 (100%)	–	–
d	10 (42.60%)	–	–	0 (28.18%)	–	–	1 (75.93%)	–	–
γ	9.70	4.91	17.12	9.41	4.68	16.84	6.80	2.96	14.28
c	8.04	7.35	8.76	14.54	5.79	15.44	2.49	0.87	4.28
ι	-1.44	-2.13	-0.81	-1.84	-4.50	0.40	-1.21	-1.72	-0.73
ρ	0.86	0.67	0.96	0.97	0.93	1.00	0.85	0.56	0.96
σ^2	0.55	0.32	0.87	0.35	0.22	0.54	0.34	0.18	0.56
δ^2	13.64	5.61	45.88	10.71	4.94	30.69	13.64	5.63	46.08
Λ	0.18	0.07	0.83	0.14	0.06	0.48	0.19	0.07	0.81

Median, 2.5%- and 97.5%-percentile of after burn-in parameter draws, conditional on the most commonly selected k and d as reported (share of total draws in parentheses). Computed from 20000 after burn-in draws for each model.

Figure 4: Posterior results for US and annual rates of change (YoY).

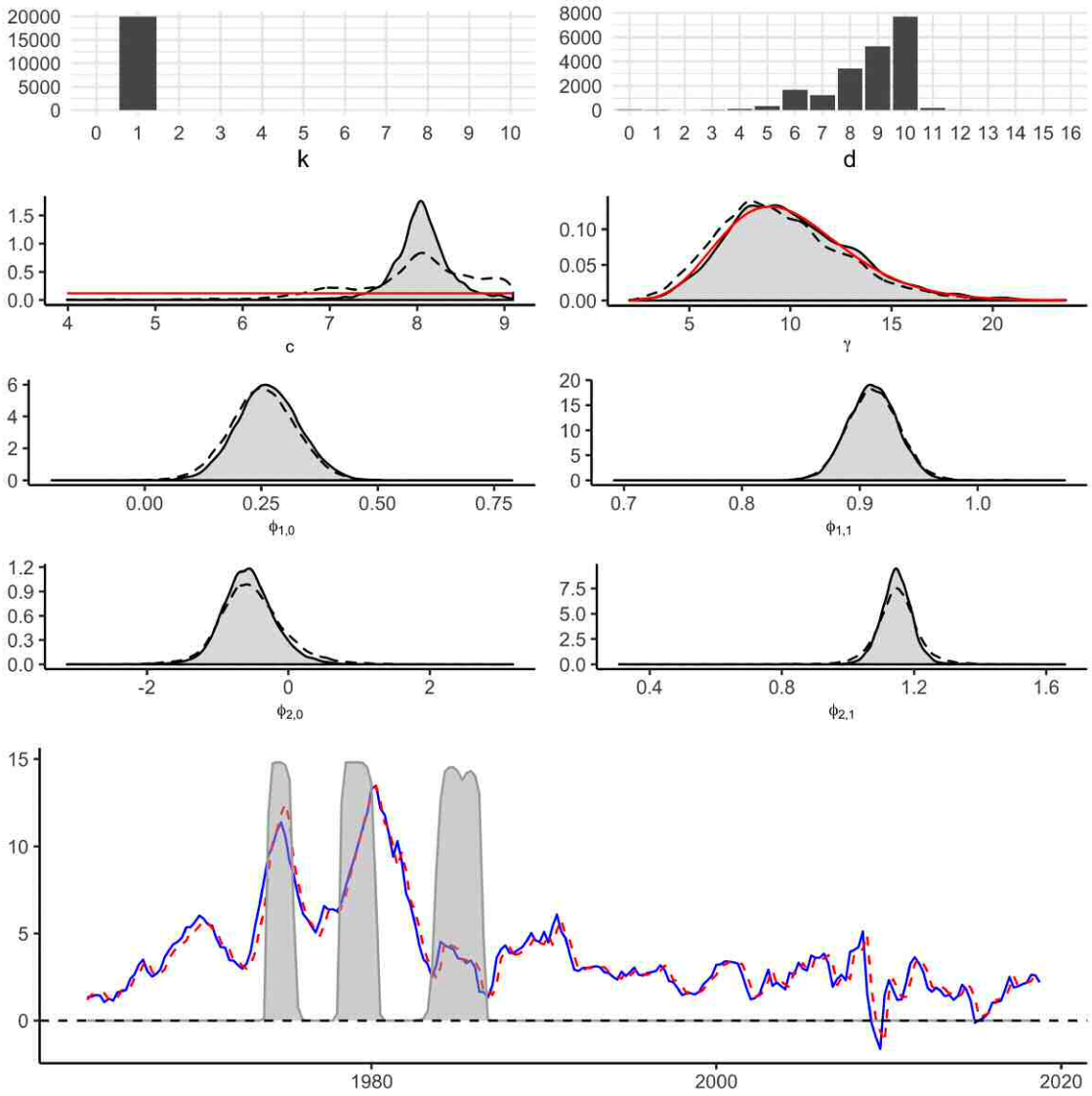

From top to bottom and left to right: (1) posterior draws for k, (2) posterior draws for d, (3)&(4) density of posterior draws for c and γ (black line and shaded area for density conditional on most commonly drawn k and d, black dashed line for unconditional density, red line prior density), (5)-(8) density of posterior draws for AR parameters $\boldsymbol{\phi}$ (black line and shaded area for density conditional on most commonly drawn k and d, black dashed line for density unconditional on d), (9) blue line inflation, dashed red line fitted inflation, dark grey line and shaded area rescaled implied transition function (conditional on most commonly drawn k and d). Computed from 20000 after burn-in draws for each model.

Figure 5: Posterior results for UK and annual rates of change (YoY).

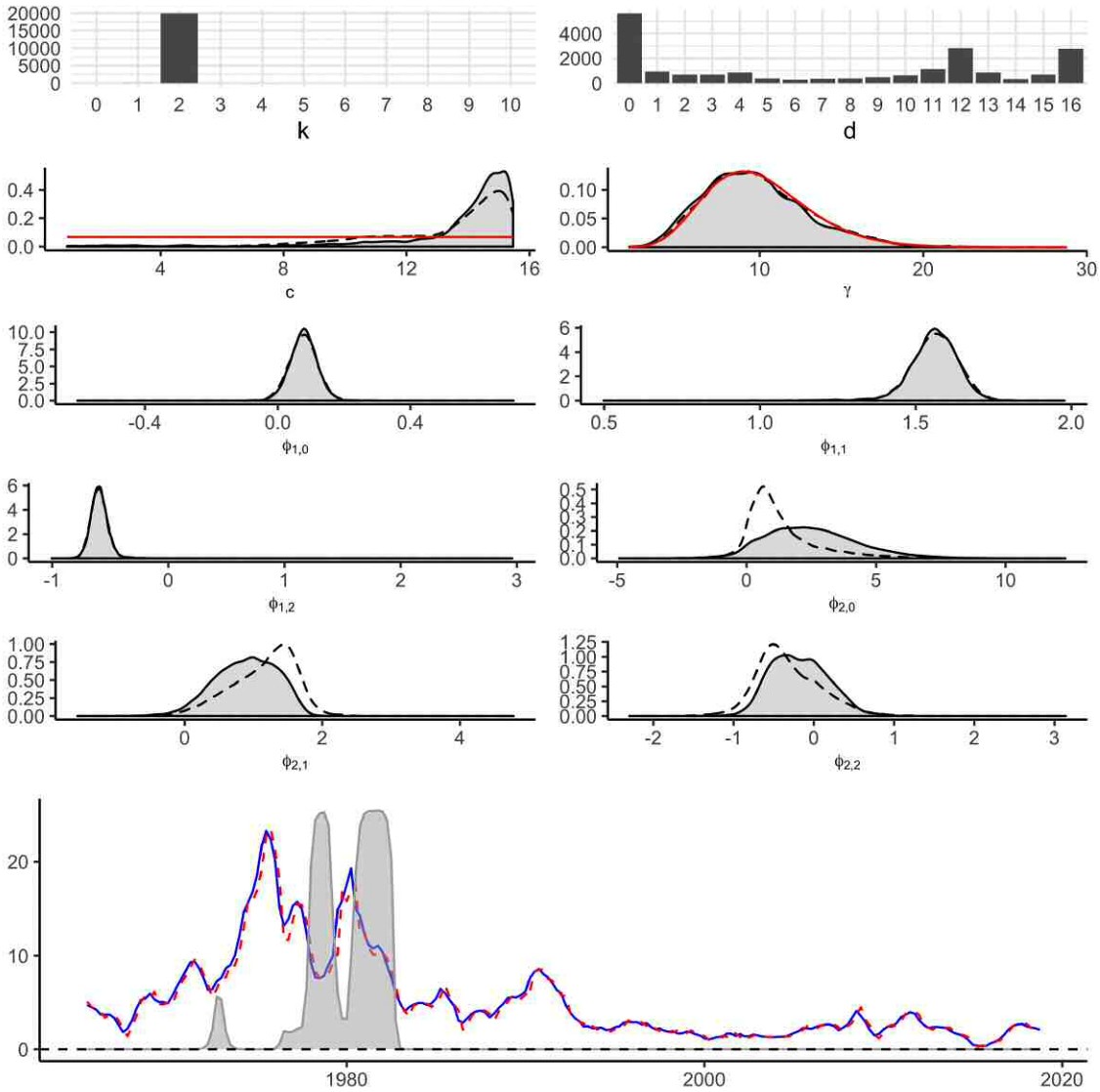

From top to bottom and left to right: (1) posterior draws for k, (2) posterior draws for d, (3)&(4) density of posterior draws for c and γ (black line and shaded area for density conditional on most commonly drawn k and d, black dashed line for unconditional density, red line prior density), (5)-(8) density of posterior draws for AR parameters $\boldsymbol{\phi}$ (black line and shaded area for density conditional on most commonly drawn k and d, black dashed line for density unconditional on d), (9) blue line inflation, dashed red line fitted inflation, dark grey line and shaded area rescaled implied transition function (conditional on most commonly drawn k and d). Computed from 20000 after burn-in draws for each model.

Figure 6: Posterior results for Canada and annual rates of change (YoY).

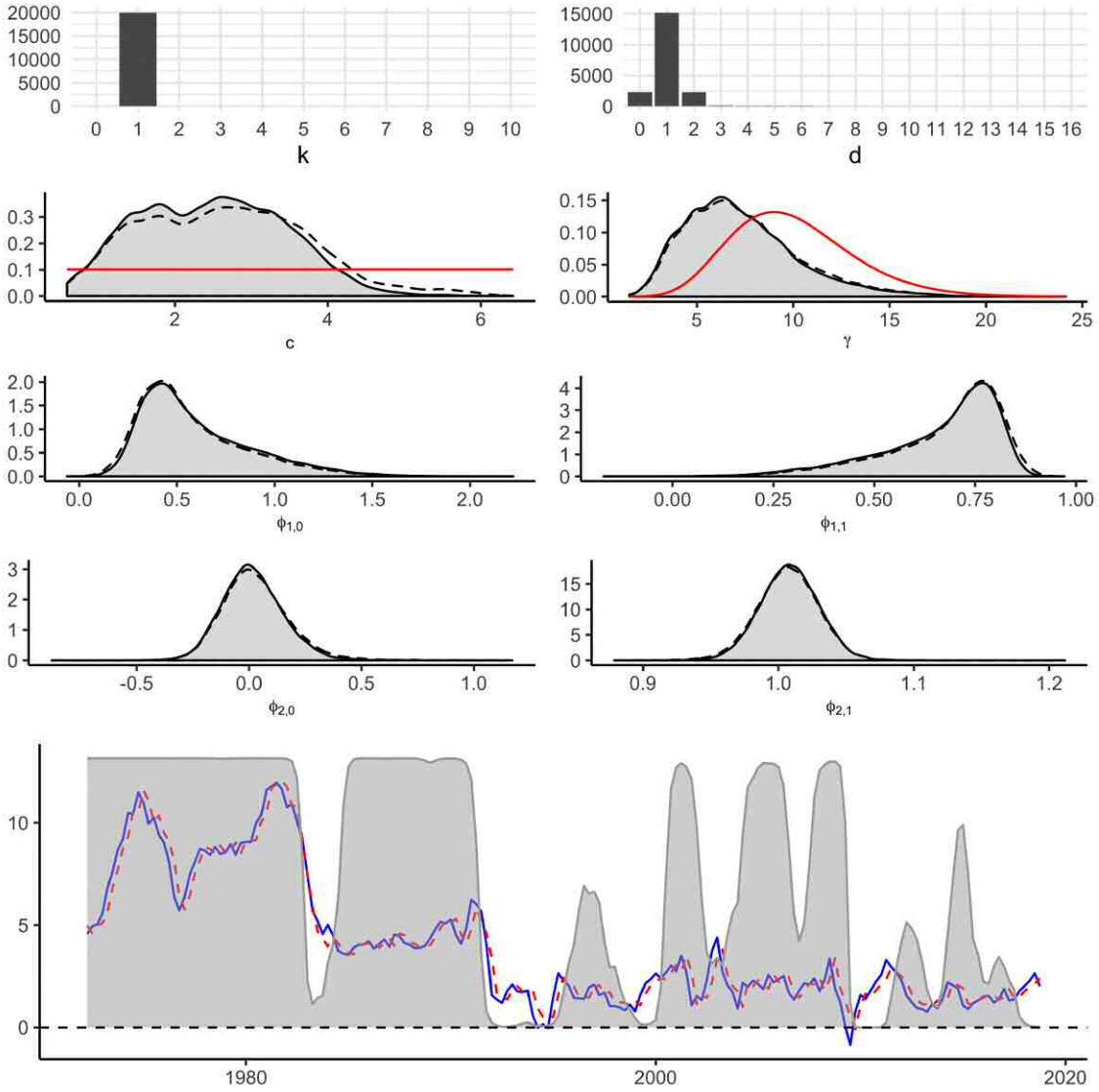

From top to bottom and left to right: (1) posterior draws for k, (2) posterior draws for d, (3)&(4) density of posterior draws for c and γ (black line and shaded area for density conditional on most commonly drawn k and d, black dashed line for unconditional density, red line prior density), (5)-(8) density of posterior draws for AR parameters $\boldsymbol{\phi}$ (black line and shaded area for density conditional on most commonly drawn k and d, black dashed line for density unconditional on d), (9) blue line inflation, dashed red line fitted inflation, dark grey line and shaded area rescaled implied transition function (conditional on most commonly drawn k and d). Computed from 20000 after burn-in draws for each model.

Starting with the lag order k, the model almost exclusively prefers a single lag order across all data sets as their posterior probability never drops below 99%. In particular, the most visited lag order is $k = 1$ in most cases, only for annual growth rates in the UK the model identifies a lag order of $k = 2$. The (almost uniformly) decisive evidence in favor of inflation as following an AR(1) process is in line with the most commonly applied lag order for modeling inflation in the literature.

In contrast, the posterior evidence on the delay parameter deserves a deeper discussion. Considering the effective prior probability for any given d is 6.25%, the posterior probabilities for the most commonly visited delay parameter range between 17.91% (Canada QoQ; Tab. A1) and 75.93% (Canada YoY; Tab. 2).

Taking a closer look, however, the posterior histograms of the delay parameter, in particular for the US and Canada, (top right panels in Fig. 4 & Fig. C.1 and Fig. 6 & Fig. C.3) reveal that the delay parameter draws are, more or less, distributed around the most commonly visited one. Yet, the posterior probability mass is spread dissimilar between each case, and more importantly, around different modes. Looking at annual rates of change, for the US almost all of the posterior draws settled in a range between 5 and 10, with $d = 10$ constituting 42.60% of total draws, while in the case of Canada, three consecutive delay parameters alone, i.e. $d = \{1, 2, 3\}$, account for almost all draws. Interestingly enough, the distributions differ substantially between the different rate of change measures. Changing the view to the quarterly measure, the most commonly drawn delay parameter for Canadian data is $d = 8$ (17.91%) with the rest of the draws unevenly petering out from there over the whole range. The disparity appears less pronounced in the case of the US, roughly 90% of posterior draws still settle between delay 5 and 10, yet, the posterior mass peaks earlier at $d = 7$ and mostly piles up on the interval 5 to 9 with over 85% of total draws. Based on UK data and annual rates of change, the model allots the most posterior draws to $d = 0$ with 28.18%, scattering the rest over the whole range with two peaks at $d = 12$ and $d = 16$, each amassing roughly 10% of the posterior draws. This rather puzzling outcome probably defies any economic explanation and is most likely either due to some artifact in the money growth indicator itself or the general lack of information on the delay in the UK data (supported by the QoQ results). Hence, based on the posterior evidence we conclude that the model limits the range of the delay parameter for the UK.

However, knowledge of the delay of the signal is only useful paired with information on how strong the signal has to be in order to trigger a regime switch. This information, of course, is contained in the posterior estimates of the threshold parameter c. The respective density plots of c show that in almost all cases the data adds concise information on the threshold parameter. Again, the results for the quarterly UK dataset shows the weakest posterior gains relative to the uniform prior, albeit a tendency to the upper end can be observed.

Especially for the US and Canada, the model identifies the threshold parameters fairly well. Yet, the threshold levels deviate between rate of change measures and across countries. This difference may partly be explained by the different monetary aggregates used for each country's money growth indicator. It is interesting to note that the estimates of the threshold parameter differ between the two growth rates measures but not consistently – it decreases for the US while increases for Canada (see Table A1. Moreover, apart from the US and annual growth rates, the posterior densities appear to be robust against the delay parameter, as their shape and location only deviate little between the conditional (on most selected d and k) and unconditional representations. Lastly, the switch from one regime to the other crucially depends on the threshold parameter relative to the transition variable. Although the posterior estimates of c appear to be fairly precise, the regime switching behaviour of the model reacts very sensitively to changes in the threshold. For instance, comparing the 95% posterior interval of the Canadian threshold parameter based on annual rates of change with the respective, underlying money growth indicator (top right panel in Figure 3) shows that the latter exceeds the lower bound of 0.87 in almost all periods. Consequently, the model would assign these periods to the high inflation regime and, in turn, signal transitory pressure much earlier than at the median or upper bound. This little exercise exemplifies that the uncertainty surrounding the threshold parameter has the potential to heavily influence the inferences drawn from the model and should not be disregarded.

Both discussed parameters are of utmost importance for policy makers. For instance, using the example of the most likely outcome in the US and annual rates of change (see Fig. 4), if the money growth indicator increases from quarter to quarter by more than 8.04%, then inflation is expected to transition to or operate in the high regime in 10 quarters ahead.[13] Since the evidence on the latter is far from decisive, a more sensible interpretation would be to consider a window of 6 to 10 quarters and to form expectations based on the respective posterior probabilities.

[13]More precisely, the most likely outcome for the threshold parameter is given by the mean of its posterior draws. Since the posterior density of the threshold parameter resembles a normal distribution, the median is reasonably close to the mean and thus the expected value of the density. The mean of the posterior distribution equals 8.05 in this case.

We now turn to the description of the assigned regimes and analyse whether the regime specific AR parameters point to distinct inflation processes. At this point it is worth recalling that the intensity of the transition crucially depends on the parameter γ. However, according to the posterior densities the data lacks valid information on the smoothing parameter (across all datasets) such that the interpretation of slowly accelerating regime switches is not supported by the data.

Starting with the US, the money growth indicator clearly identifies in both cases, annual and quarterly rates of change, the high inflation peak in the mid 70s and signals the transition to the second peak around 1980. After a short spell under the low regime, the model assigns inflation in the mid-80s to the high regime. Similarly, the money growth indicator, based on quarterly rates of change (Fig. C.1), briefly hints on inflationary pressure in the late 1990s and after the dip of the Great Recession – where the observations certainly do not command it – without fully committing to the regime switch.

For both annual and quarterly rates of change, the regime specific model parameters are well identified and, apart from the constant of the upper regime, statistically significant. Moreover, between the lower and upper regime, the AR parameters exhibit significant differences as their confidence sets do not intersect, supporting the evidence on a disparity in persistence between inflation regimes. Since the AR parameters are not restricted to be stationary, the model identifies (annual growth rates) an explosive, i.e. $\phi > 1$, process in the upper regime. Consequently, an estimated mean of inflation as defined above does not exist for the upper regime, yet, for the lower regime the state mean is defined and equals $\mu_1 = 2.96$. Interestingly enough, based on quarterly rates of change data, both state dependent means are computable and result in a lower regime oscillating around $\mu_1 = 2.79$ and a upper regime around $\mu_2 = 12.62$.[14] These results show that the transition signal from the money growth indicator implies a significant risk to price stability, as US inflation in the high regime either follows an explosive process or one that sluggishly fluctuates around almost 13%.

We continue with the UK and remind the reader that, due to the imprecise threshold and delay parameter identification, some cautious inference on UK inflation may be drawn from the estimated model parameters. First of all, for both datasets, the results imply stationary processes in both regimes with confidence. Moreover, the upper regime process is estimated to be less persistent than its counterpart both times. However, as based on annual rates, the model fails in assigning the period of highest inflation in the mid-70s to the upper regime, we turn to the quarter-on-quarter rates. With this specification, the periods assigned to the high regime capture the acceleration of inflation around 1970 as well as the phase prior to and after peak inflation in 1980. Taken together with the evidence obtained from annual rates of change, it has to be noted that the LSTAR-SV model faces some challenges to identify regime switches confidently for the UK.

For Canada, the upper regime covers almost the whole time series based on annual rates of change. While it appears economically sensible to assign the periods from the sample start to the early-80s and, to a lesser degree, the one from the mid 1980s to the early-90s to the high regime, the transition spikes, varying in intensity, from the mid 1990s onwards do not coincide with clear inflation acceleration. These are most likely the remnants of signal turned to noisiness in the money growth indicator over time. The posterior results on the model parameters indicate the upper regime follows a slightly explosive process. Consequently, the upper regime is non-stationary and the state mean is not defined. Considering quarterly rates of change, the money growth indicator assigns the high inflation period in the beginning of the sample to the mid-80s to the upper regime and, after a gap of 3 years, the medium inflation period peaking around 1990/1991. Again, the transition function spikes slightly on three occasions in the 2000s without inflation definitely demanding it.

In summary, it has been shown that the LSTAR-SV model performs well on US and Canadian data and delivers clear messages for the role of money growth for inflationary regimes. Yet, the posterior results based on both UK datasets appear less sensible and cast doubt on the suitability of the model for the UK. We conclude that the estimated threshold and delay parameters are not consistent across countries and between both rate

[14]For the upper regime, the 95% posterior confidence sets include zero for the constant, i.e. not statistically significant, as well as one and values above for the AR parameter, i.e. explosive process. For the sake of illustration, these facts are disregarded and the median case is assumed.

of change measures. The inconsistency between the former may be explained by the different monetary aggregates used in the respective money growth indicators, however, it also cautions against assuming a universal regime switching dynamic applies to inflation everywhere, as is done with regards to the delay in Amisano and Fagan (2013) who also employ the same country specific monetary aggregates. Moreover, these results may point towards a structural difference in the economies under scrutiny such that economy specific characteristics should be carefully taken into account. Nevertheless, our model successfully assigns most of the obvious high inflation periods to the upper regime. Yet, the transition functions also indicate regime switches in rather inconspicuous inflation periods. The most likely explanation is that the model primarily extracts decisive information on the parameters determining the transition, i.e. the threshold and delay parameter, from these distinctly high inflation periods early in the samples and the transition spikes later on are simply the result of noisiness in the money growth indicator randomly transgressing the constant threshold – presumably with no implication on inflation regimes. Hence, a potential model extension could try to capture structural breaks to reduce the noisiness of the signal.

Lastly, the estimates on the regime specific model parameters are in most cases well defined and support the evidence of distinct inflation regimes, distinguishable by their mean and persistence. The information contained in the processes of the upper regime are, in general, relevant for policy makers as they either follow an explosive process or oscillate persistently around high inflation means. The lower regime processes turn out to be stationary and evolve around a mean of 2 to 3%, which is in line with or reasonably close to current inflation targets.

In general, Amisano and Fagan (2013) conclude with some confidence that money growth serves as an early warning indicator for inflation, whereas our LSTAR-SV model results suggest a deeper discussion. While the evidence on when the risk of such a switch is to be expected, i.e. the delay parameter, is rather vague, we can decisively narrow down a time frame over multiple quarters rather than pinpoint a single one. In essence, our approach identifies plausible regime switches and reveals the importance of taking posterior uncertainty seriously. Especially this appears in some cases non-trivial for practical applications as well. In addition, some inconsistencies between the rate of change measures, in particular regarding the delay parameter, justifies thorough robustness checks regarding the trend-cycle decomposition, the money growth indicators, and the importance of taking heteroscedastic errors into account.

5 Robustness

Some features of the model are designed in order to avoid a priori priming the analysis on certain assumptions, e.g. the model order or delay parameter. Nonetheless, the results presented so far are still conditional on the money growth adjustment procedure detailed in Sec. 3, in particular, on (i) the decomposition method, i.e. one-sided HP filter, used to extract trend estimates for output and velocity, and (ii) the MA order $q = 5$ for smoothing, subsequent, adjusted money growth. The sensitivity of the model with regards to (i) is examined by comparing the results of several money growth indicators, each obtained on the basis of alternative filtering techniques, and the influence of (ii) is checked by computing the results with respect to different choices for q. In a second exercise, we investigate the question of heteroskedasticity and whether or not it is necessary to include, which is reported first.

5.1 Constant error variance

A key feature of the previous analysis is relaxing the assumption of homoskedasticity by allowing the error variance itself to vary over time. This is incorporated by modeling the conditional variance as an SV process. Consequently, computing the results based on the assumption of a constant conditional variance,

Table 3: Posterior estimates, all countries, annual rate of change (YoY), constant error variance.

	Annual rates of change								
	US			UK			Canada		
Parameter	$\theta_{0.5}$	$\theta_{0.025}$	$\theta_{0.975}$	$\theta_{0.5}$	$\theta_{0.025}$	$\theta_{0.975}$	$\theta_{0.5}$	$\theta_{0.025}$	$\theta_{0.975}$
$\phi_{1,0}$	0.25	0.09	0.41	0.02	-0.24	0.24	0.38	0.08	0.99
$\phi_{1,1}$	0.91	0.87	0.95	1.70	1.47	1.92	0.79	0.43	0.95
$\phi_{1,2}$	–	–	–	-0.70	-0.94	-0.44	–	–	–
$\phi_{2,0}$	-0.33	-1.26	0.52	1.93	0.95	3.89	0.13	-0.21	2.11
$\phi_{2,1}$	1.13	1.01	1.29	1.30	0.63	1.30	0.99	0.79	1.04
$\phi_{2,2}$	–	–	–	-0.48	-0.64	-0.48	–	–	–
k	1	(99.98%)	–	2	(99.62%)	–	1	(100%)	–
d	8	(23.36%)	–	0	(15.95%)	–	1	(16.68%)	–
γ	8.39	3.89	15.90	9.28	4.27	17.87	8.25	3.36	16.36
c	8.22	6.50	9.04	10.20	6.97	14.72	3.79	1.19	9.04
σ_c^2	0.42	0.35	0.51	0.55	0.44	0.69	0.38	0.31	0.49
δ^2	13.72	5.62	47.18	10.67	4.75	29.70	13.52	5.64	43.90
Λ 0.19	0.07	0.85	0.14	0.06	0.47	0.18	0.07	0.85	

Median, 2.5%- and 97.5%-percentile of after burn-in parameter draws, conditional on the most commonly selected k and d as reported (share of total draws in parentheses). Computed from 20000 after burn-in draws for each model.

i.e. $\epsilon_t \sim \mathcal{N}(0, \sigma_c^2)$, then implies replacing the step of obtaining the latent time-varying log-variance vector h with simulating draws of the constant variance parameter σ_c^2 from a conditional posterior distribution.[15]

The results obtained from the LSTAR model with constant error variance are reported in the same fashion as before in Sec. 4 for the annual rates of change while the results based on quarterly data can be found in Sec. D.1. Taking a look at Fig. 7 (and Fig. D.1) first, however, gives some indication on whether heteroskedasticity is present in the data. For each country, the plots depict how the median of time-varying variance, i.e. $exp(\boldsymbol{h})$ evolves over time against the median as well as the 95% posterior set of σ_c^2, essentially illustrating what is implied by a constant error variance. Both figures reveal time-varying variance exceeds the upper confidence bound of σ_c^2, in parts excessively, over several periods, i.e. during the 2000s in the US, from the early-70s to mid-80s in the UK, and, on four occasions in Canada, while being considerable lower than its 2.5% confidence bound over the rest of the times series. However, allowing for heteroscedasticity appears necessary as the plots indicate strongly for the US and UK, as well, to a lesser degree, for Canada. The posterior results of the SV parameters in Tab. 2 (and Tab. A1) corroborate this evidence, as the data added significant information to their priors.[16]

The developing picture shows, that the results obtained with the LSTAR-SV model are, generally, in line with the ones from the LSTAR model. Specifically, the model order k, the model parameters $\boldsymbol{\phi}$, the implicit parameters of the transition function γ and c, as well as the hyperparameters are similar in terms of sign and magnitude. Yet, the LSTAR-SV model seems to produce more precise estimates. Moreover, the LSTAR model with constant error variance evidently performs much worse with regards to the delay parameter. The posterior share of the most selected delay never exceeds 23.36% and is particularly atrocious in case of quarterly rate of change data, where the posterior probability of the most drawn parameter exceeds its effective prior probability merely by 1-2%. Having said that, for each dataset, the transition function,

[15]This means, in particular, replacing the second step of the Gibbs sampling scheme specified in **??** and conditioning the following steps on σ_c^2 instead of the SV model parameters. The prior for σ_c^2 is chosen to be of conjugate form, $\sigma_c^2 \sim \mathcal{IG}\alpha_{\sigma_c^2}, \beta_{\sigma_c^2}$. Moreover, the posterior derivations in Sec. A.1 still apply by setting each element of $\boldsymbol{h}$ to $h_t = \sigma_c^2$.

[16]Additional results comparable to the figures in the previous Sec. 4 can be obtained from the authors upon request.

Figure 7: Time-varying versus constant error variance, all countries, annual rates of change.

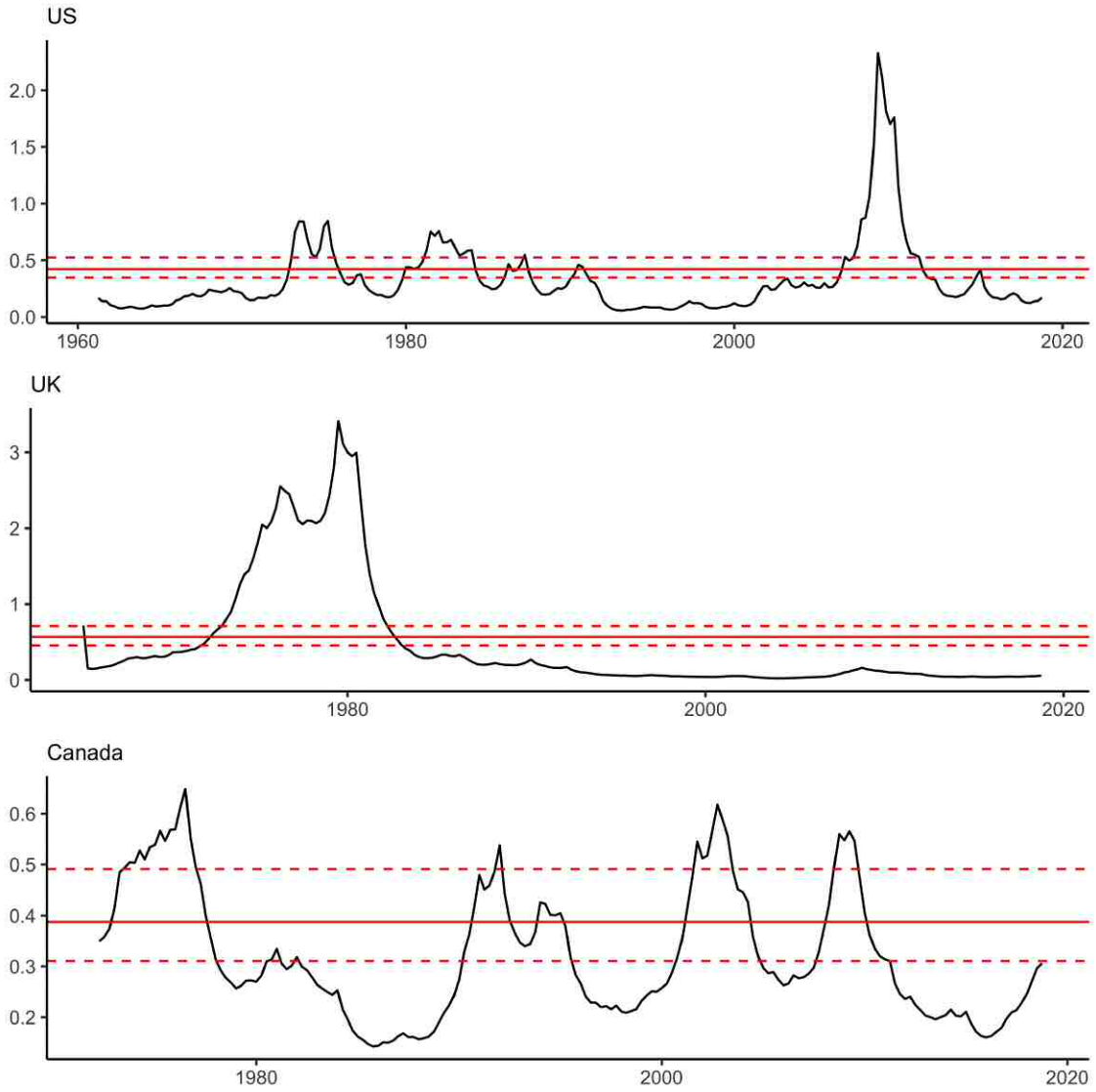

Median of posterior draws for time-varying variance, i.e. $exp(\boldsymbol{h})$, (black line), horizontal lines imply median (red line) and 95% confidence set (red dashed line) of posterior draws for constant error variance σ_c^2. Plots corresponding to : US, UK, Canada (from top to bottom). Computed from 20000 after burn-in draws for each model.

conditional on the most selected d and k as well as the medians of c and γ, assigns almost the same periods to the upper regime as the corresponding transition function of the LSTAR-SV model.

In summary, comparing time-varying with constant conditional variance suggests that heteroskedasticity is present in the errors produced by the conditional mean (LSTAR) model applied to inflation. Furthermore, it has been shown that the effect of assuming constant variance instead leads to less precise but similar posterior estimates, with the exception of the delay parameter. Nonetheless, both models identify similar periods belonging to the high inflation regime in each dataset. Hence, allowing for heteroskedasticity in the LSTAR framework by incorporating the SV model improves the precision of the estimates, in particular for the delay parameter d which is in particular a desireable feature for policy makers.

5.2 Money Growth Indicator

The investigation regarding the impact of the money growth adjustment procedure is two-fold. First, the robustness of the model against the MA(q) order, used for smoothing adjusted money growth, is checked by comparing the results computed for a range of values for q from 3 to 7, where $q = 5$ corresponds to the specification of the main findings. Secondly, the robustness against alternative trend decomposition techniques in the money growth adjustment procedure is separately examined as well. The set of filter methods contains the (i) augmented one-sided HP (main findings), (ii) augmented two-sided HP, (iii) rolling window, and (iv) Hamilton regression type filter as well as (v) the raw money growth. As already pointed out in Sec. 3.2, the rolling window and Hamilton filter consume a considerable amount of observations to obtain similar trends, hence, their datasets carry less observations than their counterparts. In order to condition the analysis on the same amount of information, the results for each filter type are computed from the same amount of data, i.e the intersection of the set of alternative money growth indicators for each country.

All things considered, each exercise requires the estimation of 3 (countries) $\times$ 2 (rate of change measures) $\times$ 5 (different filter/MA orders) = 30 models. For the interested reader, the results are comprehensively reported for the YoY specification in Tab. A2 & Tab. A3 in the appendix which present the posterior outputs, conditional on the most selected k and d, for each model.[17] In both exercises, apart from the implicit parameters, the results are largely consistent with each other. Hence, Fig. D.4 & Fig. D.5 in the appendix show – for each country and rate of change measure – combined histograms of all filter types for d and combined density plots for the threshold c. To concisely summarize the most important information carried by the implicit parameters, i.e. when does the transition function imply regime switches, the heatmaps in Fig. 8 (and in Fig. D.3) report the following. Each cell corresponds to one quarter and is colored according to the value of the transition function F_t at time t, for each filter type or MA(q) order, respectively. Regarding alternative filter types, the heatmaps indicate very mixed results. In particular, the patterns evident in the heatmaps for the UK and Canada (annual rate of change; see Figure 8), are distinctly different between the models (or groups of models), implying that the models assign periods to the upper regime inconsistently.

[17] As the picture remains qualitatively unchanged for quarterly rates of change, we do not report the results here but provide them upon request.

Figure 8: Heatmap of transition function values F_t based on alternative filtering techniques, annual rate of change.

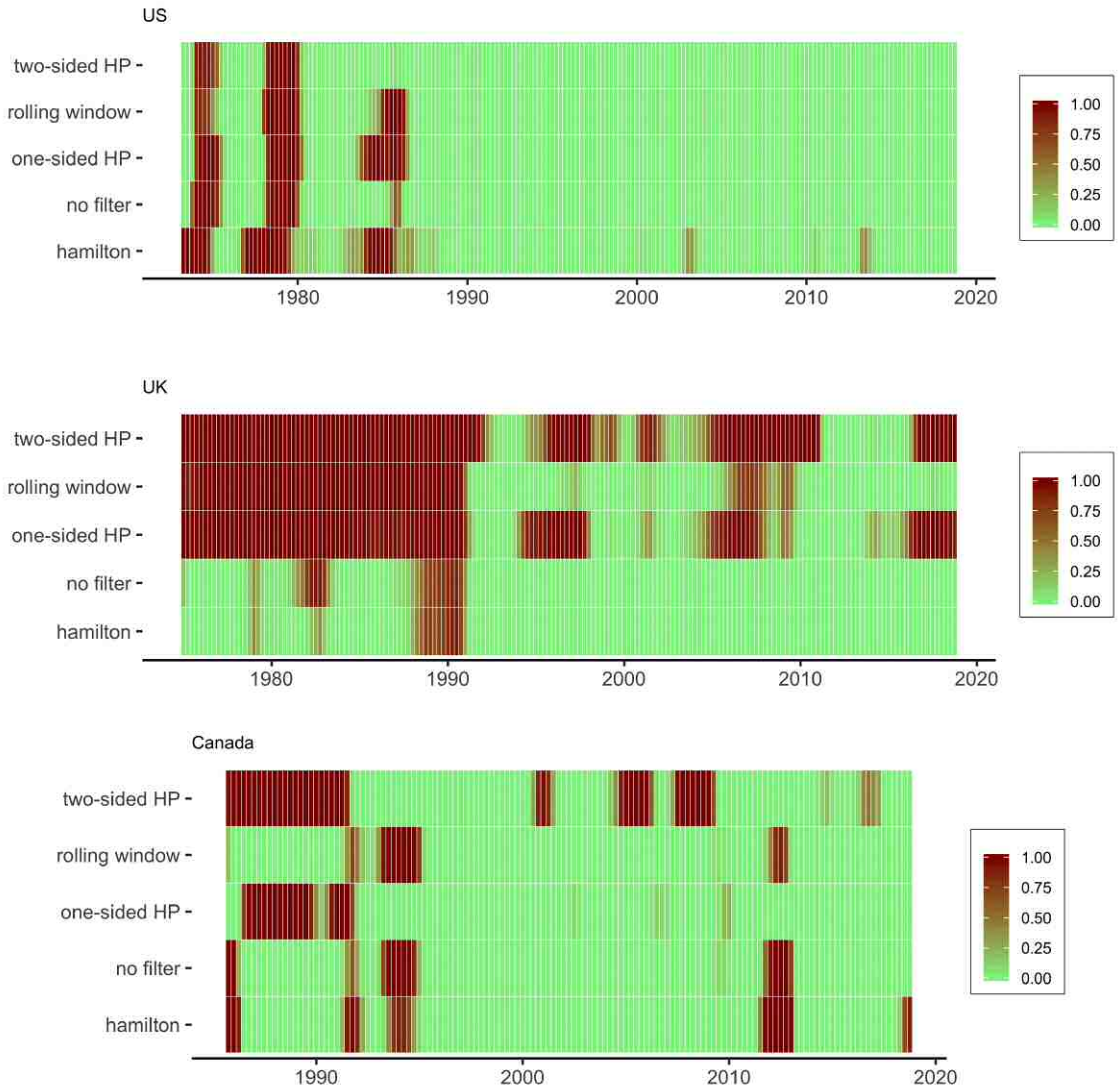

Each cell corresponds to one quarter. Color transitions from $F_t = 0$ (lightgreen) to $F_t = 1$ (darkred). F_t computed from median values, conditional on most commonly selected k and d for each model. Plots corresponding to: US, UK, Canada (from top to bottom). Computed from 20000 after burn-in draws for each model.

Inspecting the heatmaps, generated by transition functions of the models based on different MA(q) orders, on the other hand, reveals in almost all cases quite similar patterns, which mostly deviate only slightly with regards to the intensity, length, or start of the upper inflation regime.

Figure 9: Heatmap of transition function values based on different MA(q) orders, annual rate of change.

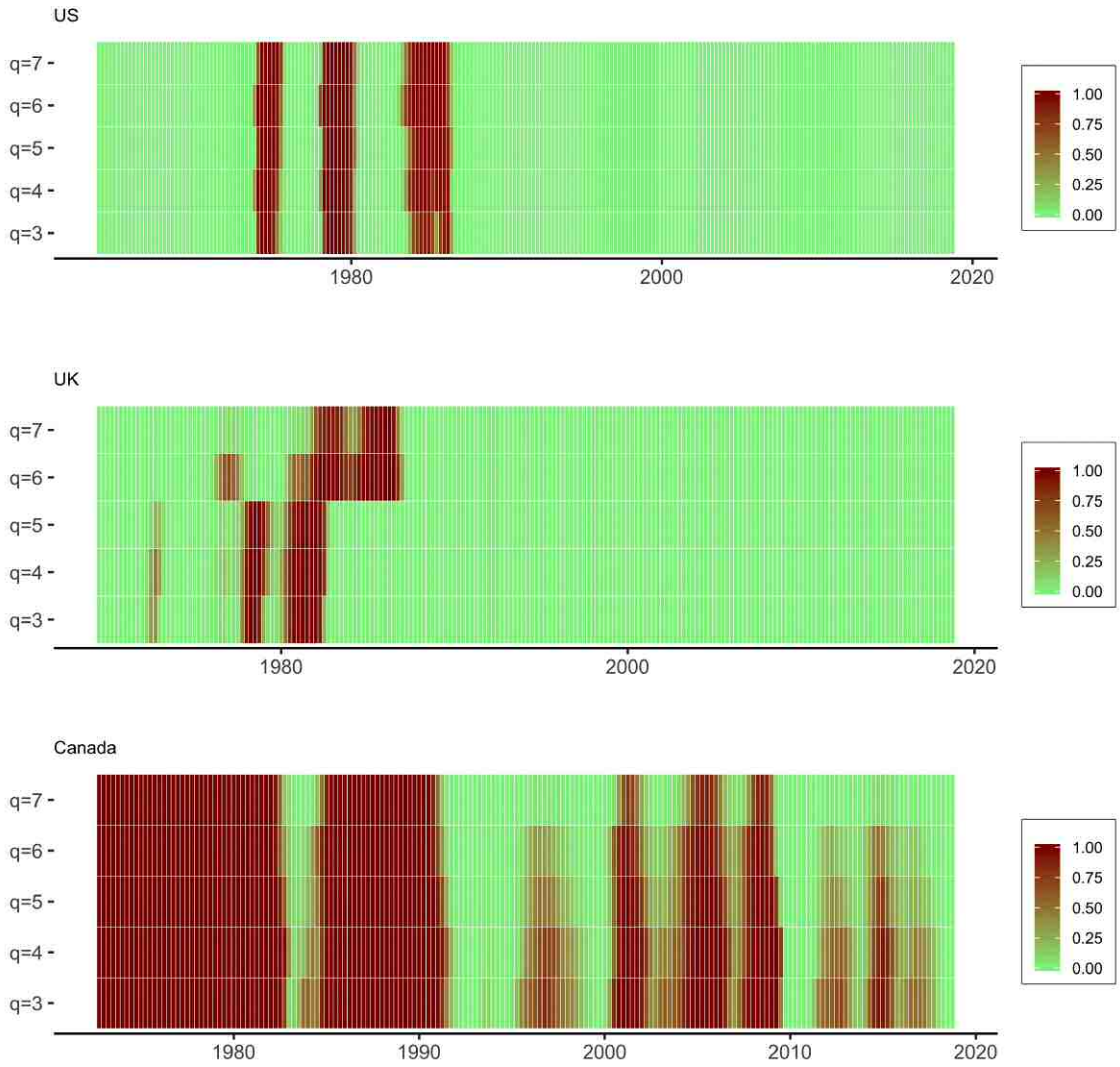

Each cell corresponds to one quarter. Color transitions from $F_t = 0$ (lightgreen) to $F_t = 1$ (darkred). F_t computed from median values, conditional on most commonly selected k and d for each model. Plots corresponding to: US, UK, Canada (from top to bottom). Computed from 20000 after burn-in draws for each model.

Summarizing, testing the robustness of the LSTAR-SV model against alternative filter types has produced evidence, that the implicit parameters are particularly sensitive to the specific choice of the trend decomposition method – in the worst cases, leading to ambiguous early warning signals. The second exercise, however, indicates that models based on different MA(q) orders assign similar periods to the upper regime. This means, the results are fairly robust with regards to the MA(q) order, however, some deviations are still present. Again policymakers interested in the role of money growth for inflationary regimes need to decide carefully about the specific money growth adjustment procedure. In particular, capturing the remaining uncertainty with regards to q, for instance, could be achieved by different methods like Bayesian Model Averaging.

6 Concluding remarks

Recent developments have put a sizable question mark on the once firm and well-established linkage between money growth and inflation. Discarding the notion of the former directly predicting the latter, Amisano and Fagan (2013) showed in a Markov Switching setting how money growth may play a role in shifting inflation regimes. The present paper follows the same line by modeling inflation as a two-state Logistic Smooth Transition Autoregressive (LSTAR) process, in which the transition from a low to high inflation regime is triggered by lagged money growth – adjusted for long-run trends in output and velocity – transgressing a threshold parameter.

Drawing from a considerable amount of literature, a fully Bayesian analysis of the LSTAR model is presented, which allows the model order and the delay of the money growth signal to be estimated as parameters. Furthermore, the standard assumption of homoskedasticity has been relaxed by incorporating a Stochastic Volatility model for the error variance, leading to improved precision of the parameters. The resulting LSTAR-SV model is applied to quarterly data from the US, the UK and Canada. The model successfully identifies well-known high inflation periods in the samples, largely supporting the findings in Amisano and Fagan (2013) that money growth signals transitory pressure in inflation. Additionally, our findings produce evidence on the correct delay of this signal, which turns out to be non-universal but rather economy specific. For instance, the money growth signal in the US leads inflation regimes 5 to 10 quarters ahead, while in the UK most evidence points to it translating immediately. As suspected, the identified regimes exhibit differences in mean and persistence, which imply relevant dynamics for policy makers. The lower regimes mostly oscillate around a mean of 2-3% – in line with or close to common inflation targets – and the upper regime either evolves sluggishly around a mean upwards of 8% or follows an explosive process.

Several observations, however, have revealed that the robustness of the model is susceptible to (i) the growth measure analyzed, (ii) the trend decomposition method, and, to a lesser extent, (iii) the degree of adjusted money growth smoothing. Thus, our results suggest that policy makers should carefully assess theses issues when implementing money growth as early warning indicator for price stability distortions.

Moreover, the threshold parameter appears to be sometimes driven by well-known high inflation periods of the 70s and 80s, and some signals indicating inflationary pressure later on appear to be outliers of signal turned to noisiness with little implication for (or necessity from) inflation. Hence, further research could thus consist of incorporating some form of structural breaks, like a time-varying threshold parameter, into the presented analysis of the LSTAR-SV model.

While our results do support the role of money growth as an indicator of regime switches in inflation, it appears worthwhile to explore the money growth adjustment procedure further, in particular providing a theoretical foundation of the underlying trend decomposition. This may alleviate the problem of model uncertainty such that LSTAR-SV approach could help to assess risks to inflation for policy makers even more reliable.

References

AMISANO G, AND FAGAN G (2013), "Money growth and inflation: A regime switching approach," *Journal of International Money and Finance* **33**(C), 118–145. [2, 3, 6, 7, 8, 9, 12, 20, 26, 32]

ASSENMACHER-WESCHE K, AND GERLACH S (2008), "Interpreting euro area inflation at high and low frequencies," *European Economic Review* **52**(6), 964 – 986. [2]

BANK OF ENGLAND (2019), "Quarterly amounts outstanding of M4 (monetary financial institutions' sterling M4 liabilities to private sector) (in sterling millions) seasonally adjusted [LPQAUYN]," Retrieved from Bank of England Database; September 10, 2019. [32]

BENATI L (2008), "Investigating Inflation Persistence across Monetary Regimes," *The Quarterly Journal of Economics* **123**(3), 1005–1060. [2]

BLOECHL A (2014), "Reducing the Excess Variability of the Hodrick-Prescott Filter by Flexible Penalization," Discussion Papers in Economics 17940, University of Munich, Department of Economics. [8]

BOARD OF GOVERNORS OF THE FEDERAL RESERVE SYSTEM (US) (2019), "M2 Money Stock [M2SL]," Retrieved from FRED, Federal Reserve Bank of St. Louis; September 10, 2019. [32]

BORDO MD, AND ORPHANIDES A (2013), *Introduction to*, University of Chicago Press. [2]

BRAZIER A, HARRISON R, KING M, AND YATES T (2008), "The Danger of Inflating Expectations of Macroeconomic Stability: Heuristic Switching in an Overlapping-Generations Monetary Model," *International Journal of Central Banking* **4**(2), 219–254. [2, 4]

COGLEY T, AND SARGENT T (2001), "Evolving post World War II US inflation dynamics," *NBER Macroeconomics Annual* **16**, 331–373. [4]

COGLEY T, AND SARGENT TJ (2005), "Drifts and volatilities: monetary policies and outcomes in the post WWII US," *Review of Economic dynamics* **8**(2), 262–302. [4]

DESCHAMPS PJ (2008), "Comparing smooth transition and Markov switching autoregressive models of US unemployment," *Journal of Applied Econometrics* **23**(4), 435–462. [6]

FAUST J, AND WRIGHT JH (2013), "Chapter 1 - Forecasting Inflation," in G ELLIOTT, AND A TIMMERMANN (eds.) "Handbook of Economic Forecasting," *Handbook of Economic Forecasting*, volume 2, 2 – 56, Elsevier. [9]

FRIEDMAN M (1963), *Inflation: Causes and Consequences*, Asia Publishing House. [2]

GEFANG D, AND STRACHAN R (2009), "Nonlinear Impacts of International Business Cycles on the U.K. – A Bayesian Smooth Transition VAR Approach," *Studies in Nonlinear Dynamics Econometrics* **14**(1), 1–33. [6]

GEMAN S, AND GEMAN D (1984), "Stochastic Relaxation, Gibbs Distributions, and the Bayesian Restoration of Images," *IEEE Transactions on Pattern Analysis and Machine Intelligence* **PAMI-6**(6), 721–741. [7]

GEORGE DA, AND OXLEY L (2008), "Money and inflation in a nonlinear model," *Mathematics and Computers in Simulation* **78**(2), 257 – 265. [2]

GERLACH R, AND CHEN CWS (2008), "Bayesian inference and model comparison for asymmetric smooth transition heteroskedastic models," *Statistics and Computing* **18**(4), 391. [4]

GREEN PJ (1995), "Reversible jump Markov chain Monte Carlo computation and Bayesian model determination," *Biometrika* **82**(4), 711–732. [7, 30]

GÜRKAYNAK RS, LEVIN A, AND SWANSON E (2010), "Does Inflation Targeting Anchor Long-Run Inflation Expectations? Evidence from the U.S., UK, and Sweden," *Journal of the European Economic Association* **8**(6), 1208–1242. [2]

HAMILTON JD (2018), "Why You Should Never Use the Hodrick-Prescott Filter," *The Review of Economics and Statistics* **100**(5), 831–843. [8, 12]

HANSEN BE (2011), "Threshold autoregression in economics," *Statistics and its Interface* **4**(2), 123–127. [3]

HODRICK RJ, AND PRESCOTT EC (1997), "Postwar U.S. Business Cycles: An Empirical Investigation," *Journal of Money, Credit and Banking* **29**(1), 1–16. [8]

KASTNER G (2016), "Dealing with Stochastic Volatility in Time Series Using the R Package stochvol," *Journal of*

Statistical Software **69**(5), 1–30. [7]

KASTNER G, AND FRÜHWIRTH-SCHNATTER S (2014), "Ancillarity-sufficiency interweaving strategy (ASIS) for boosting MCMC estimation of stochastic volatility models," *Computational Statistics Data Analysis* **76**, 408 – 423. [4]

KAUFMANN S (2015), "K-state switching models with time-varying transition distributions—Does loan growth signal stronger effects of variables on inflation?" *Journal of Econometrics* **187**(1), 82 – 94. [2]

KIM S, SHEPHARD N, AND CHIB S (1998), "Stochastic Volatility: Likelihood Inference and Comparison with ARCH Models," *The Review of Economic Studies* **65**(3), 361–393. [4]

KING RG, AND REBELO ST (1993), "Low frequency filtering and real business cycles," *Journal of Economic Dynamics and Control* **17**(1), 207 – 231. [8]

LIU JS, LIANG F, AND WONG WH (2000), "The Multiple-Try Method and Local Optimization in Metropolis Sampling," *Journal of the American Statistical Association* **95**(449), 121–134. [7, 30]

LIVINGSTON G, AND NUR D (2017), "Bayesian inference for smooth transition autoregressive (STAR) model: A prior sensitivity analysis," *Communications in Statistics - Simulation and Computation* **46**(7), 5440–5461. [13]

LOPES HF, AND SALAZAR E (2006), "Bayesian Model Uncertainty In Smooth Transition Autoregressions," *Journal of Time Series Analysis* **27**(1), 99–117. [3, 5, 7]

LUBRANO M (2000), *Bayesian analysis of nonlinear time series models with a threshold*, 61–78, Cambridge University Press. [6]

MARAVALL A, AND DEL RÍO A (2007), "Temporal aggregation, systematic sampling, and the Hodrick–Prescott filter," *Computational Statistics Data Analysis* **52**(2), 975 – 998. [8, 9]

OECD (2019a), "Consumer Price Index of All Items in the United Kingdom [GBRCPIALLMINMEI]," Retrieved from FRED, Federal Reserve Bank of St. Louis; September 10, 2019. [32]

——— (2019b), "M3 for Canada [MABMM301CAQ189S]," Retrieved from FRED, Federal Reserve Bank of St. Louis;, September 10, 2019. [32]

OFFICE FOR NATIONAL STATISTICS (2019a), "Gross domestic product at market prices:Implied deflator:SA; Source dataset: GDP first quarterly estimate time series [PN2]," Retrieved from Office for National Statistics; September 10, 2019. [32]

——— (2019b), "Gross Domestic Product: chained volume measures: Seasonally adjusted £m; Source dataset: GDP first quarterly estimate time series [PN2]," Retrieved from Office for National Statistics; September 10, 2019. [32]

ORPHANIDES A, AND PORTER R (2001), *Money and inflation: the role of information regarding the determinants of M2 behaviour*, 77–97, European Central Bank. [8, 32]

RITTER C, AND TANNER MA (1992), "Facilitating the Gibbs Sampler: The Gibbs Stopper and the Griddy-Gibbs Sampler," *Journal of the American Statistical Association* **87**(419), 861–868. [7]

SARGENT TJ, AND SURICO P (2011), "Two Illustrations of the Quantity Theory of Money: Breakdowns and Revivals," *The American Economic Review* **101**(1), 109–128. [2]

SARNO L, TAYLOR MP, AND PEEL DA (2003), "Nonlinear Equilibrium Correction in U.S. Real Money Balances, 1869-1997," *Journal of Money, Credit and Banking* **35**(5), 787–799. [2]

SIMS CA (2001), "[Evolving Post-World War II U.S. Inflation Dynamics]: Comment," *NBER Macroeconomics Annual* **16**, 373–379. [3, 4]

STATISTICS CANADA (2019a), "Table 18-10-0004-01 Consumer Price Index, monthly, not seasonally adjusted," Retrieved from Statstics Canada;September 10, 2019. [32]

——— (2019b), "Table 36-10-0104-01 Gross domestic product, expenditure-based, Canada, quarterly (x 1,000,000)," Retrieved from Statstics Canada; September 10, 2019. [32]

——— (2019c), "Table 36-10-0106-01 Gross domestic product price indexes, quarterly," Retrieved from Statstics Canada; September 10, 2019. [32]

STOCK JH, AND WATSON M (2006), "Chapter 10 - Forecasting with Many Predictors," *Handbook of Economic Forecasting*, volume 1, 515–554, Elsevier, 1 edition. [9]

STOCK JH, AND WATSON MW (1999), "Forecasting inflation," *Journal of Monetary Economics* **44**(2), 293 – 335. [8]

——— (2007), "Why Has U.S. Inflation Become Harder to Forecast?" *Journal of Money, Credit and Banking* **39**(1), 3–33. [2]

TAYLOR SJ (1982), "Financial returns modelled by the product of two stochastic processes-A study of the daily sugar prices 1961-75," *Time Series Analysis : Theory and Practice* **1**, 203–226. [3]

TERÄSVIRTA T (1994), "Specification, Estimation, and Evaluation of Smooth Transition Autoregressive Models," *Journal of the American Statistical Association* **89**(425), 208–218. [3, 6]

TONG H, AND LIM KS (1980), "Threshold Autoregression, Limit Cycles and Cyclical Data," *Journal of the Royal Statistical Society. Series B (Methodological)* **42**(3), 245–292. [3]

TROUGHTON P, AND GODSILL SJ (1998), "A reversible jump sampler for autoregressive time series," in "Proceedings of the 1998 IEEE International Conference on Acoustics, Speech and Signal Processing, ICASSP '98 (Cat. No.98CH36181)," volume 4, 2257–2260. [7]

US BUREAU OF ECONOMIC ANALYSIS (2019a), "Gross Domestic Product: Implicit Price Deflator [GDPDEF]," Retrieved from FRED, Federal Reserve Bank of St. Louis; September 10, 2019. [32]

——— (2019b), "Real Gross Domestic Product [GDPC1]," Retrieved from FRED, Federal Reserve Bank of St. Louis; September 10, 2019. [32]

US BUREAU OF LABOR STATISTICS (2019), "Consumer Price Index: All Items in U.S. City Average, All Urban Consumers [CPIAUCSL]," Retrieved from FRED, Federal Reserve Bank of St. Louis; September 10, 2019. [32]

VAN DIJK D, TERÄSVIRTA T, AND FRANSES PH (2002), "Smooth Transition Autoregressive Models — A Survey of Recent Developments," *Econometric Reviews* **21**(1), 1–47. [3, 4]

VERMAAK J, ANDRIEU C, DOUCET A, AND GODSILL SJ (2004), "Reversible Jump Markov Chain Monte Carlo Strategies for Bayesian Model Selection in Autoregressive Processes," *Journal of Time Series Analysis* **25**(6), 785–809. [5, 6, 7]

WOODFORD M (1994), *Nonstandard Indicators for Monetary Policy: Can Their Usefulness Be Judged from Forecasting Regressions?*, 95–115, The University of Chicago Press. [2]

Appendix A Bayesian Estimation

A.1 Posterior Simulation

The derivation of the relevant acceptance probabilities for the Reversible-Jump MCMC (RJMCMC; Green (1995)) algorithm, yields following structure of the RJMCMC-step:

(i) Propose a new model order from the discretized Laplace density $q(k^*|k)$, where $k = k^{i-1}$;

(ii) Calculate the acceptance probability r_{RJ} as derived above;

(iii) Simulate $u \sim \mathcal{U}(0,1)$:

  (a) If $r_{RJ} > u$, set $k^i = k^*$;

  (b) Else, set $k^i = k^{i-1}$;

The Multiple-Try-Metropolis Acceptance Probability (MTM; Liu *et al.* (2000)) algorithm deviates from the standard MH algorithm by allowing several candidates to be proposed in each iteration instead of one. The structure of the MTM-step is as follows:

(i) Propose k_{MTM} trial values from $q(\gamma^*|\gamma^{(i-1)})$ and $q(c^*|c^{(i-1)})$, where $\gamma^*|\gamma^{(i-1)} \sim \mathcal{G}\left(\frac{(\gamma^{(i-1)})^2}{\Delta_\gamma}, \frac{(\gamma^{(i-1)})}{\Delta_\gamma}\right)$ and $c^*|c^{(i-1)} \sim \mathcal{TN}(c^{(i-1)}, \Delta_c)$, for $a_c \leq c^* \leq b_c$,, and form the trial set $\{\boldsymbol{\omega}_1^* = (\gamma_1^*, c_1^*), \ldots, \boldsymbol{\omega}_{k_{MTM}}^* = (\gamma_{k_{MTM}}^*, c_{k_{MTM}}^*)\}$;

(ii) Select a combination $\boldsymbol{\omega}^* = (\gamma^*, c^*)$ from $\{\boldsymbol{\omega}_1^*, \ldots, \boldsymbol{\omega}_{k_{MTM}}^*\}$ with probability $p_\omega = \frac{w(\omega^*, \omega^{(i-1)})}{\sum_{j=1}^{k_{MTM}} w(\omega_j^*, \omega^{(i-1)})}$;

(iii) Draw $k_{MTM} - 1$ values from $q(\gamma'|\gamma^*)$ and $q(c'|c^*)$, and form the set $\{\boldsymbol{\psi}_1 = (\gamma_1', c_1'), \ldots, \boldsymbol{\psi}_{k_{MTM}-1} = (\gamma_{k_{MTM}-1}', c_{k_{MTM}-1}'), \boldsymbol{\psi}_{k_{MTM}} = (\gamma^{(i-1)}, c^{(i-1)})\}$;

(iv) Calculate the acceptance probability $r_{MTM} = min\left(1, \frac{\pi(\omega^*) q(\omega^{(i-1)}|\omega^*) p_{\boldsymbol{\psi}}}{\pi(\omega^{(i-1)}) q(\omega^*|\omega^{(i-1)}) p_\omega}\right)$;

(v) Simulate $u \sim \mathcal{U}(0,1)$:

  (a) If $r_{MTM} > u$, set $\gamma^i = \gamma^*$ and $c^i = c^*$;

  (b) Else, set $\gamma^i = \gamma^{i-1}$ and $c^i = c^{i-1}$;

Posterior inference is carried out by iteratively drawing from the relevant conditional posterior distributions and discarding the first set of draws as burn-in. The Gibbs sampling scheme is laid out in detail below:

(i) Initialize $\{\boldsymbol{\phi}^{(0)}, \delta^{2(0)}, \gamma^{(0)}, c^{(0)}, d^{(0)}, k^{(0)}, \Lambda^{(0)}; \iota^{(0)}, \rho^{(0)}, \sigma^{2(0)}\}$ either deterministically or randomly and set $i = 1$;

(ii) Obtain the latent time-varying log-variance vector h^i with a call to the `'svsample2'` function in the R package `'stochvol'` at state $\{\boldsymbol{\phi}^{(i)}, \delta^{2(i-1)}, \gamma^{(i-1)}, c^{(i-1)}, d^{(i-1)}, k^{(i-1)}, \Lambda^{(i-1)}\}$;

(iii) Draw the model order $k^{(i)}$, the coefficient vector $\boldsymbol{\phi}^{(i)}$;

  (a) Simulate the model order with the RJMCMC algorithm using $p(k, \boldsymbol{\phi}|\boldsymbol{y}, \delta^{2(i-1)}, \gamma^{(i-1)}, c^{(i-1)}, d^{(i-1)}, \Lambda^{(i-1)}; \iota^{(i-1)}, \rho^{(i-1)}, \sigma^{2(i-1)})$;

(b) Draw the coefficient vector $\boldsymbol{\phi}^{(i)}|\boldsymbol{y}, \delta^{2(i-1)}, \gamma^{(i-1)}, c^{(i-1)}, d^{(i-1)}, k^{(i)}, \Lambda^{(i-1)}; \iota^{(i-1)}, \rho^{(i-1)}, \sigma^{2(i-1)}$ from $\boldsymbol{\mathcal{N}}(\hat{\boldsymbol{\phi}}, \boldsymbol{C}_{\boldsymbol{\phi}})$;

(iv) Draw $d^{(i)}$ from $p(d|\boldsymbol{y}, \boldsymbol{\phi}^{(i)}, \delta^{2(i-1)}, \gamma^{(i-1)}, c^{(i-1)}, k^{(i)}, \Lambda^{(i-1)}; \iota^{(i)}, \rho^{(i)}, \sigma^{2(i)})$

(v) Simulate the implicit parameters with the MTM algorithm using $p(\gamma, c|\boldsymbol{y}, \boldsymbol{\phi}^{(i)}, \delta^{2(i-1)}, d^{(i)}, k^{(i)}, \Lambda^{(i-1)}; \iota^{(i)}, \rho^{(i)}, \sigma^{2(i)})$;

(vi) Draw the coefficient hyperparamater $\delta^{2(i)}|\boldsymbol{y}, \boldsymbol{\phi}^{(i)}, \gamma^{(i)}, c^{(i)}, d^{(i-1)}, k^{(i)}, \Lambda^{(i-1)}; \iota^{(i)}, \rho^{(i)}, \sigma^{2(i)}$ from $\mathcal{IG}(\bar{\alpha}_{\delta^2}, \bar{\beta}_{\delta^2})$;

(vii) Draw the model order hyperparameter $\Lambda^{(i)}|\boldsymbol{y}, \boldsymbol{\phi}^{(i)}, \delta^{2(i)}, \gamma^{(i)}, c^{(i)}, d^{(i)}, k^{(i)}; \iota^{(i)}, \rho^{(i)}, \sigma^{2(i)}$ from $\mathcal{G}(\alpha_\Lambda + k^{(i)}\tau_k, \beta_\Lambda)$;

(viii) Set $i = i+1$. Replicate Steps 2 to 7 for a suitable amount of iterations, i.e. until the MCMC chains converge, then STOP.

Appendix B Data and Data Transformations

B.1 Data Sources US

The original data sources for the US analysis are as follows:

(i) CPI from U.S. Bureau of Economic Analysis (2019b)
(ii) M2 from U.S. Bureau of Labor Statistics (2019)
(iii) GDP from Board of Governors of the Federal Reserve System (US) (2019)
(iv) Deflator from U.S. Bureau of Economic Analysis (2019a)

B.2 Data Sources UK

The the data sources for the UK analysis are as follows:

(i) CPI from OECD (2019a)
(ii) M4 from Bank of England (2019)
(iii) GDP from Office for National Statistics (2019b)
(iv) Deflator from Office for National Statistics (2019a)

The price index for the UK was sourced from the OECD, since the official price index in the UK underwent several changes from retail price index (RPI) to CPI and finally harmonized consumer price index (HICP). The original monthly price index series was subject to seasonally adjustment by X-13ARIMA-SEATS and then quarterly aggregation by average.

B.3 Data Sources Canada

The data sources for Canada analysis are as follows:

(i) CPI from Statistics Canada (2019a)
(ii) M3 from OECD (2019b)
(iii) GDP from Statistics Canada (2019b)
(iv) Deflator from Statistics Canada (2019c)

The original monthly price index series was subject to seasonally adjustment by X-13ARIMA-SEATS and then quarterly aggregation by average.

B.4 Money growth indicator

The approach follows Amisano and Fagan (2013) where raw money growth is adjusted in an attempt to obtain a money growth measure, which accounts for shifts in trend in such a way that it can still be computed in real-time. A more complete discussion on this topic and its rationale is given in Orphanides and Porter (2001). Starting with the quantity theory of money in its equation of exchange form

$$M_t V_t = P_t Y_t, \tag{A.1}$$

where – at time t each – M_t is the respective money aggregate, P_t the price index, V_t velocity of income, i.e. $P_t Y_t / M_t$, and Y_t real output. Taking logs and first difference (A.1), defining $\Delta x_t = log(X_t) - log(X_{t-1})$, one obtains the equation of exchange in growth rates

$$\Delta m_t + \Delta v_t = \Delta p_t + \Delta y_t. \tag{A.2}$$

Rearranging the above in terms of inflation Δp_t yields

$$\Delta p_t = \Delta m_t + \Delta v_t - \Delta y_t. \tag{A.3}$$

The identity in equation (A.3) shows that inflationary pressure may not be indicated by raw money growth alone. Assuming the cyclical components of output and velocity growth tends to zero over medium to long horizons, money growth has to be adjusted for the trend component of both.

B.5 Different detrending methods

The top and middle panels in Fig. B.2 to Fig. B.6 report the results for each country and rate of change type. The unfiltered growth rates are also included for the sake of comparison, while the bottom panel plots the implied money growth indicators for each filter against inflation. All filter types were fed with the same full range of observations, however, as already stated, the rolling window and the Hamilton filter consume observations at the beginning of the sample for estimation. For the sake of comparability, the time frame considered in the reported figures as well as the estimations is set to their intersection. In addition, the effects of omitting some notably high inflation observations from the sample on the parameter estimates can be examined as well.

B.5.1 Annual (YoY) rates

Figure B.1: Output and velocity trend growth at annual (YoY) rates based on different filtering techniques for the US.

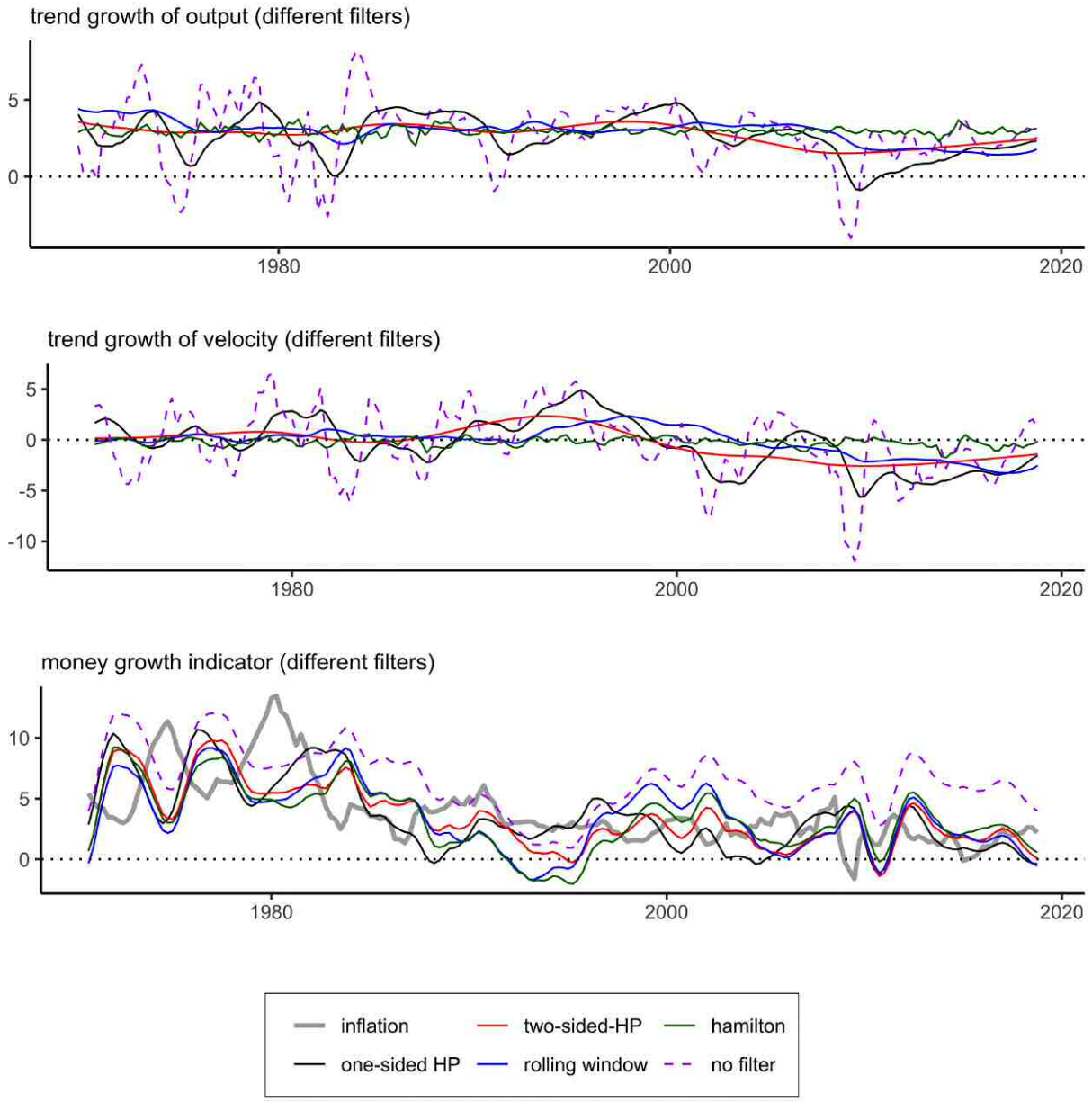

Top panel: trend estimates for output growth $\tilde{y}$. Middle panel: trend estimates for velocity growth $\tilde{v}$. Bottom panel: implied MA(5) smoothed money growth indicators Δm_t^*.

Figure B.2: Output and velocity trend growth at annual (YoY) rates based on different filtering techniques for the UK.

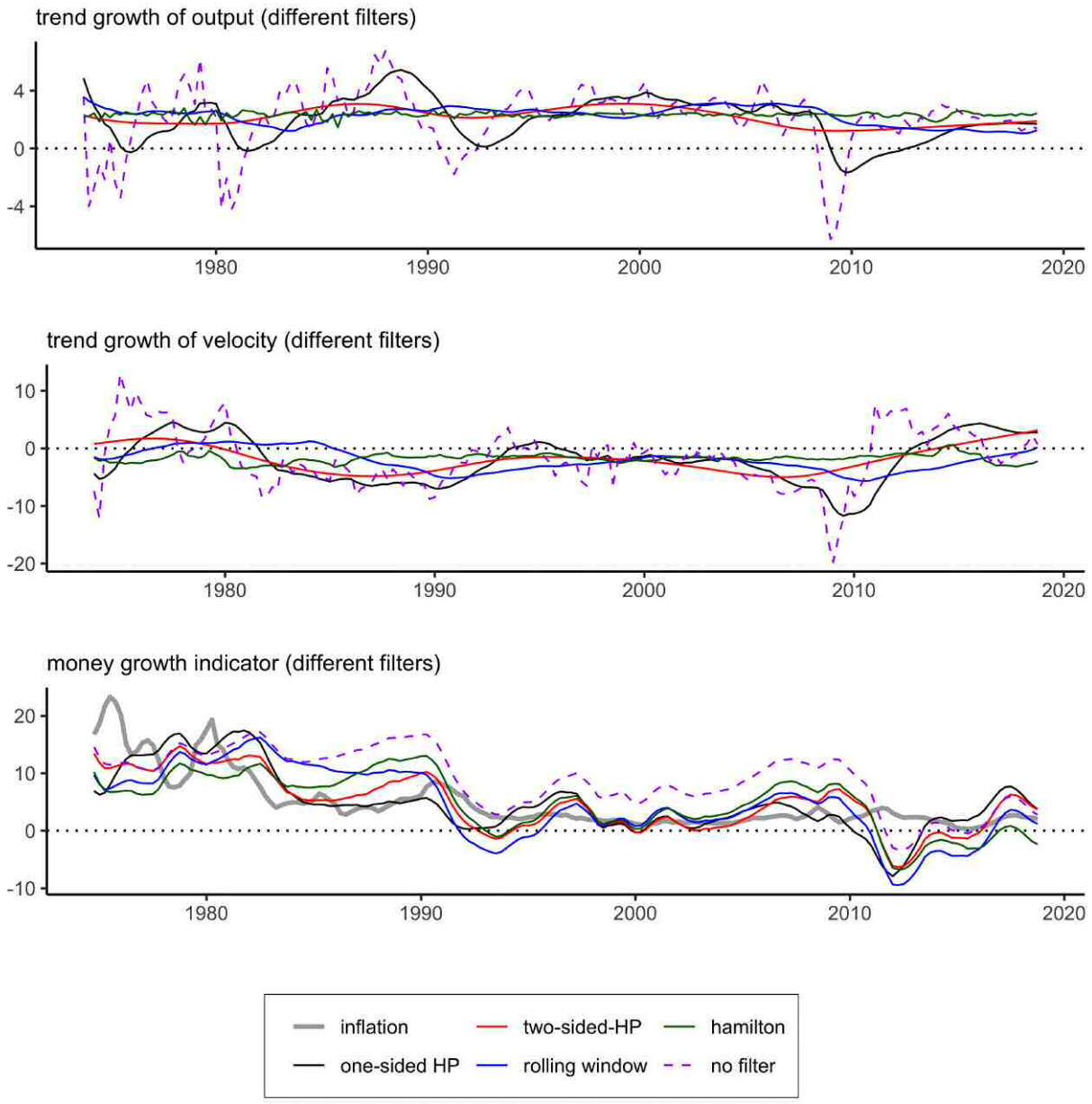

Top panel: trend estimates for output growth $\tilde{y}$. Middle panel: trend estimates for velocity growth $\tilde{v}$. Bottom panel: implied MA(5) smoothed money growth indicators Δm_t^*.

Figure B.3: Output and velocity trend growth at annual (YoY) rates based on different filtering techniques for Canada.

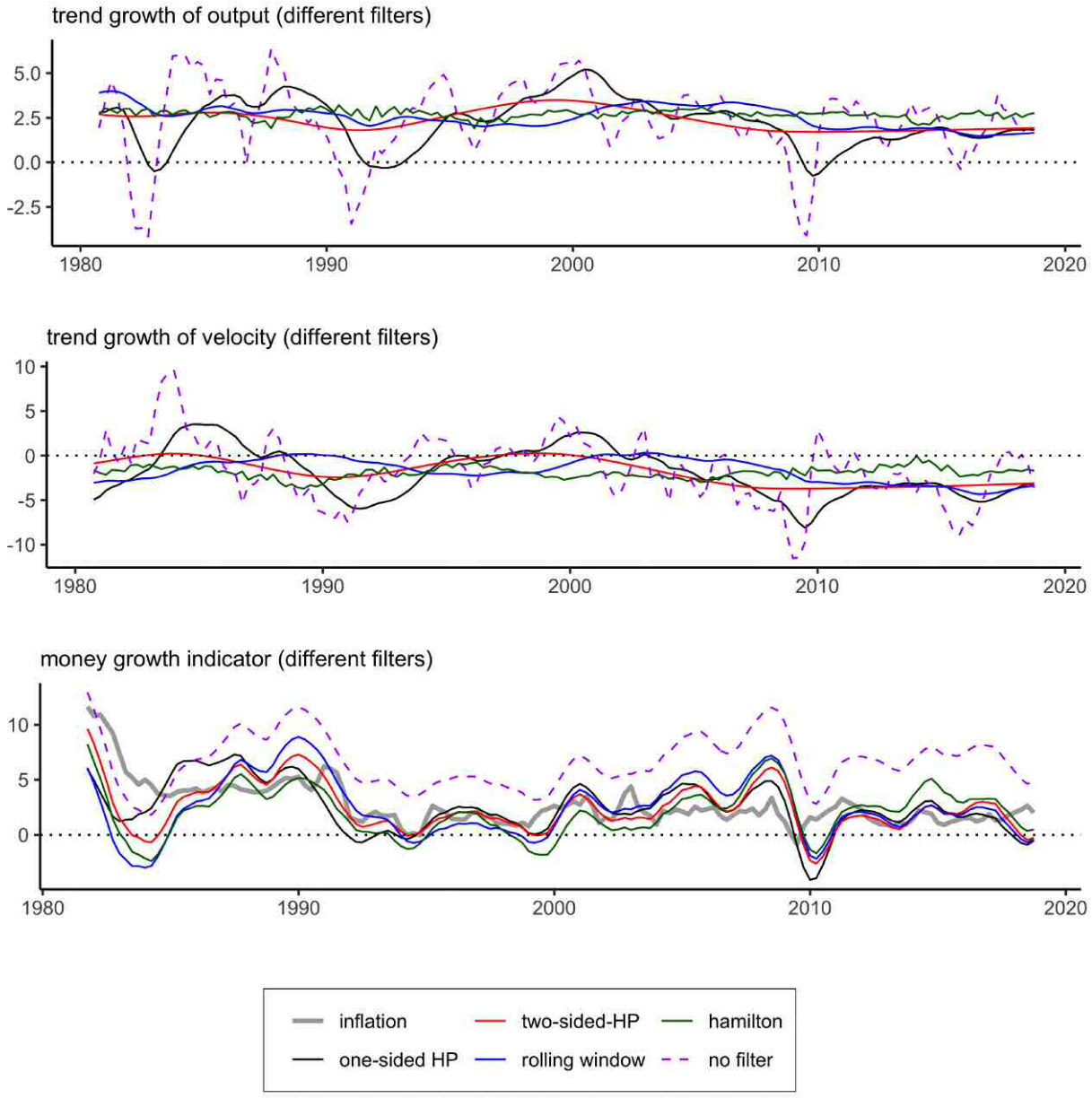

Top panel: trend estimates for output growth $\tilde{y}$. Middle panel: trend estimates for velocity growth $\tilde{v}$. Bottom panel: implied MA(5) smoothed money growth indicators Δm_t^*.

B.5.2 Quarterly (QoQ) rates

Figure B.4: Output and velocity trend growth at quarterly (QoQ) rates based on different filtering techniques for the US.

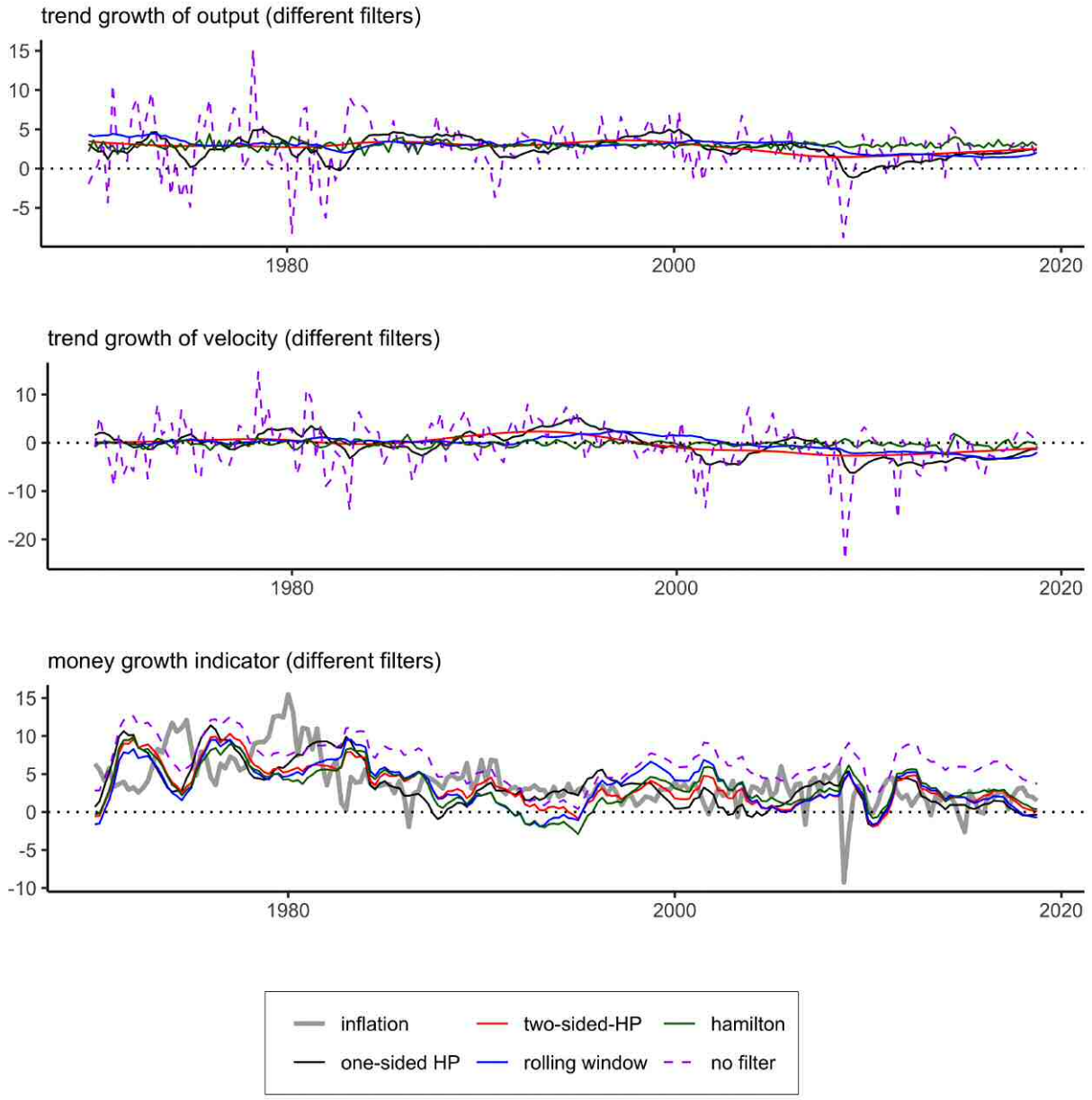

Top panel: trend estimates for output growth $\tilde{y}$. Middle panel: trend estimates for velocity growth $\tilde{v}$. Bottom panel: implied MA(5) smoothed money growth indicators Δm_t^*.

Figure B.5: Output and velocity trend growth at quarterly (QoQ) rates based on different filtering techniques for the UK.

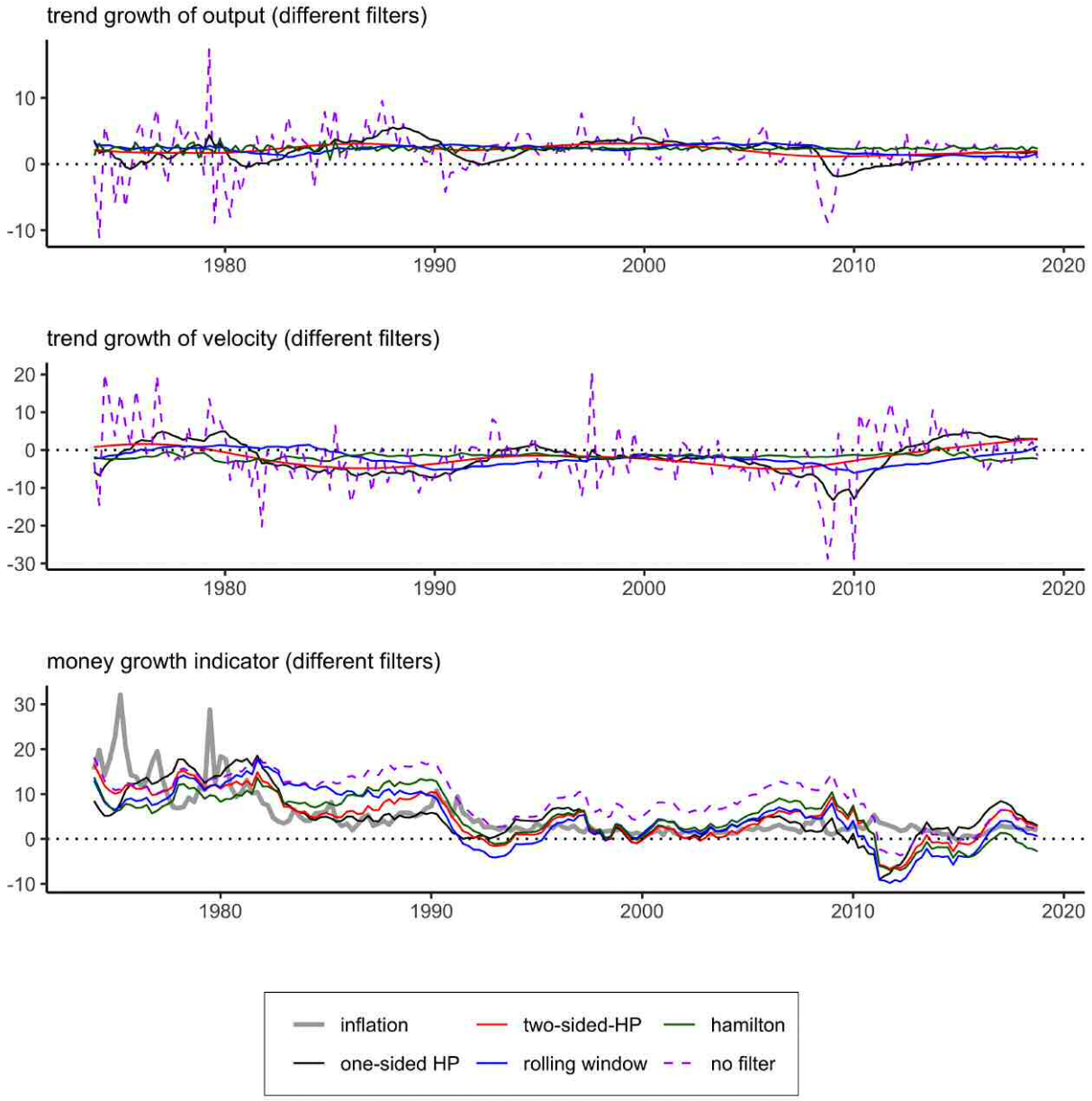

Top panel: trend estimates for output growth $\tilde{y}$. Middle panel: trend estimates for velocity growth $\tilde{v}$. Bottom panel: implied MA(5) smoothed money growth indicators Δm_t^*.

Figure B.6: Output and velocity trend growth at quarterly (QoQ) rates based on different filtering techniques for Canada.

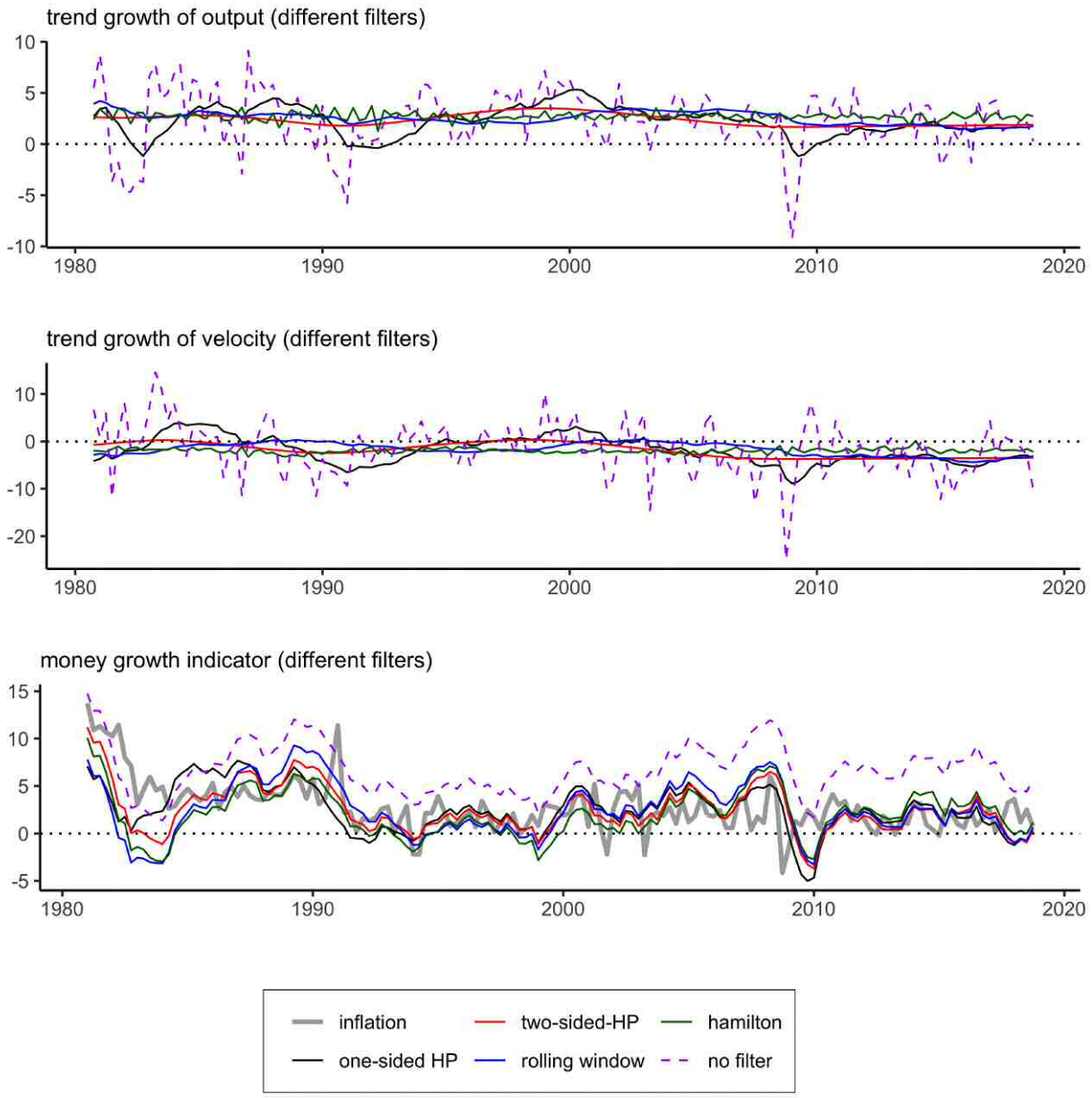

Top panel: trend estimates for output growth $\tilde{y}$. Middle panel: trend estimates for velocity growth $\tilde{v}$. Bottom panel: implied MA(5) smoothed money growth indicators Δm_t^*.

Appendix C Additional results for the QoQ specification

C.1 Additional results for the QoQ specification

Following Tab. A1 reports the median, 2.5%- and 97.5%-percentiles of the posterior distributions for each of the parameters being estimated, conditional on the most commonly drawn lag order k and delay parameter d. For each country, the results reported below are based on quarterly rates of change measures, raw money growth adjusted for output, and velocity trends obtained from the augmented one-sided HP filter. The effective sample starts are then 1960Q2 for the US, 1964Q2 for the UK, and 1971Q2 for Canada. Fig. C.1 to Fig. 3 report the results in the same fashion as in the text.

Table A1: Posterior estimates, all countries, annualized quarterly rates of change (QoQ).

	Quarterly rates of change								
	US			UK			Canada		
Parameter	$\theta_{0.5}$	$\theta_{0.025}$	$\theta_{0.975}$	$\theta_{0.5}$	$\theta_{0.025}$	$\theta_{0.975}$	$\theta_{0.5}$	$\theta_{0.025}$	$\theta_{0.975}$
$\phi_{1,0}$	1.12	0.69	1.62	0.31	0.08	0.59	1.37	0.82	1.90
$\phi_{1,1}$	0.60	0.43	0.74	0.85	0.69	0.95	0.28	0.05	0.52
$\phi_{2,0}$	0.78	-0.50	2.06	3.60	0.23	10.32	1.31	0.43	2.62
$\phi_{2,1}$	0.94	0.77	1.15	0.58	-0.03	0.94	0.82	0.66	0.94
k	1 (99.97%)	–	–	1 (99.95%)	–	–	1 (100%)	–	–
d	7 (23.96%)	–	–	0 (21.30%)	–	–	8 (17.91%)	–	–
γ	8.78	4.12	16.47	9.12	4.10	16.53	9.24	4.22	17.39
c	5.09	3.35	7.94	10.50	2.98	15.40	4.49	2.93	5.63
ι	0.68	0.08	1.27	0.25	-2.26	2.22	1.01	0.62	1.40
ρ	0.88	0.70	0.97	0.97	0.91	1.00	0.73	0.28	0.94
σ^2	0.45	0.28	0.70	0.39	0.26	0.58	0.44	0.22	0.72
δ^2	13.59	5.68	44.86	13.54	5.86	45.88	13.53	5.71	47.49
Λ	0.19	0.07	0.79	0.19	0.07	0.77	0.19	0.07	0.81

Median, 2.5%- and 97.5%-percentile of after burn-in parameter draws, conditional on the most commonly selected k and d as reported (share of total draws in parentheses). Computed from 20000 after burn-in draws for each model. Source: own results.

Figure C.1: Posterior results for US and annualized quarterly rates of change (QoQ).

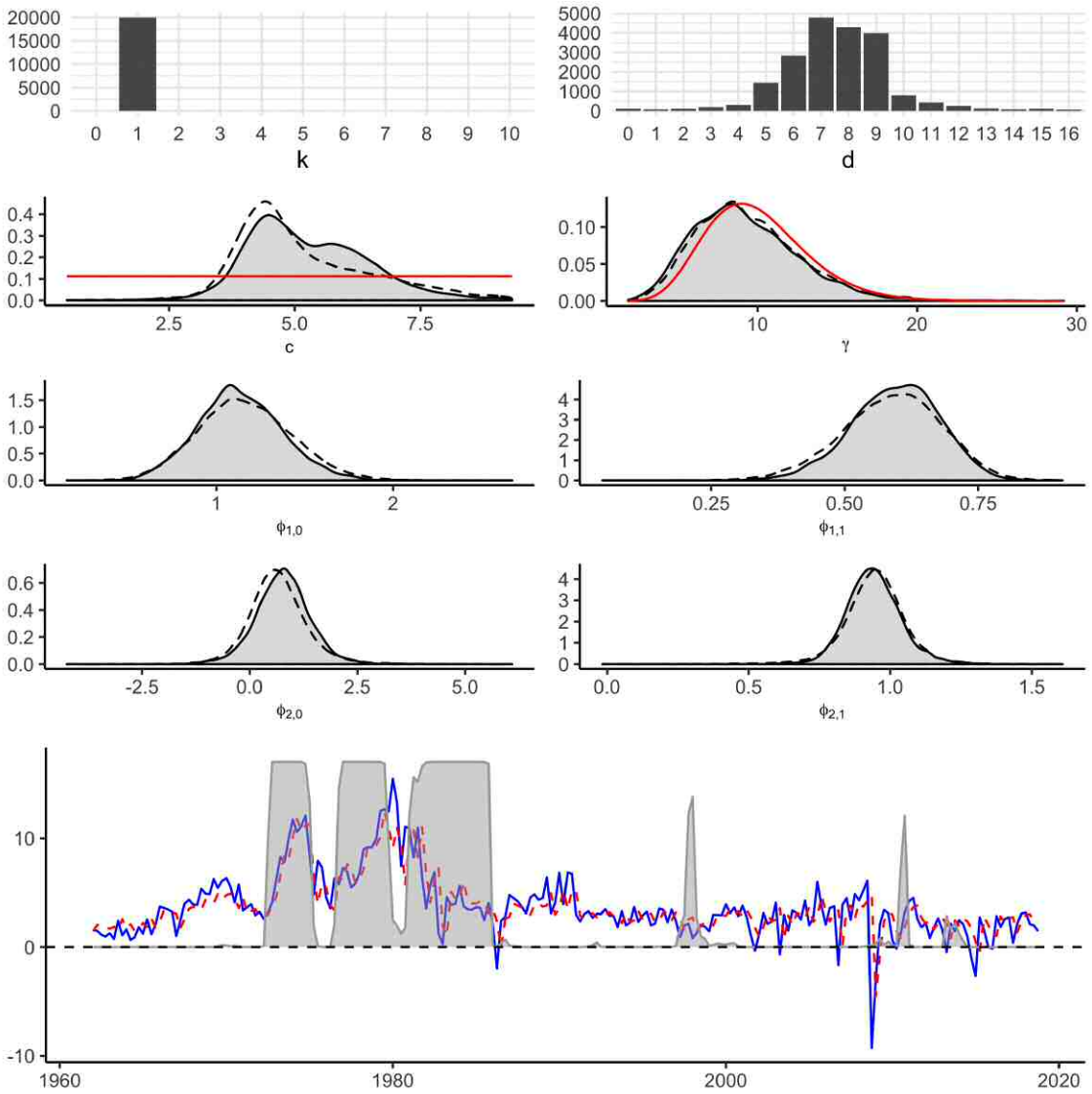

From top to bottom and left to right: (1) posterior draws for k, (2) posterior draws for d, (3)&(4) density of posterior draws for c and γ (black line and shaded area for density conditional on most commonly drawn k and d, black dashed line for unconditional density, red line prior density), (5)-(8) density of posterior draws for AR parameters $\boldsymbol{\phi}$ (black line and shaded area for density conditional on most commonly drawn k and d, black dashed line for density unconditional on d), (9) blue line inflation, dashed red line fitted inflation, dark grey line and shaded area rescaled implied transition function (conditional on most commonly drawn k and d). Computed from 20000 after burn-in draws for each model.

Figure C.2: Posterior results for UK and annualized quarterly rates of change (QoQ).

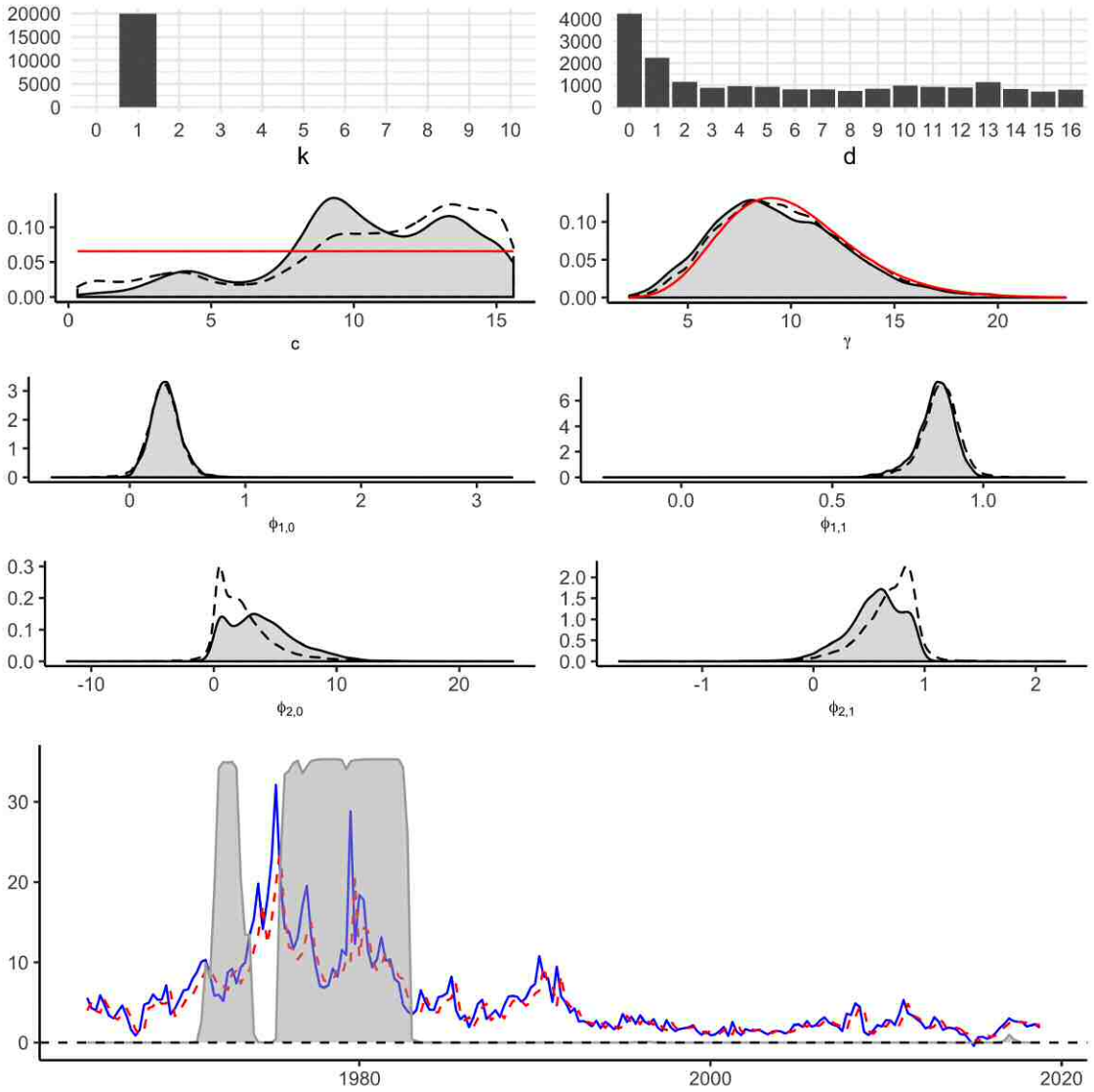

From top to bottom and left to right: (1) posterior draws for k, (2) posterior draws for d, (3)&(4) density of posterior draws for c and γ (black line and shaded area for density conditional on most commonly drawn k and d, black dashed line for unconditional density, red line prior density), (5)-(8) density of posterior draws for AR parameters $\boldsymbol{\phi}$ (black line and shaded area for density conditional on most commonly drawn k and d, black dashed line for density unconditional on d), (9) blue line inflation, dashed red line fitted inflation, dark grey line and shaded area rescaled implied transition function (conditional on most commonly drawn k and d). Computed from 20000 after burn-in draws for each model.

Figure C.3: Posterior results for Canada and annualized quarterly rates of change (QoQ).

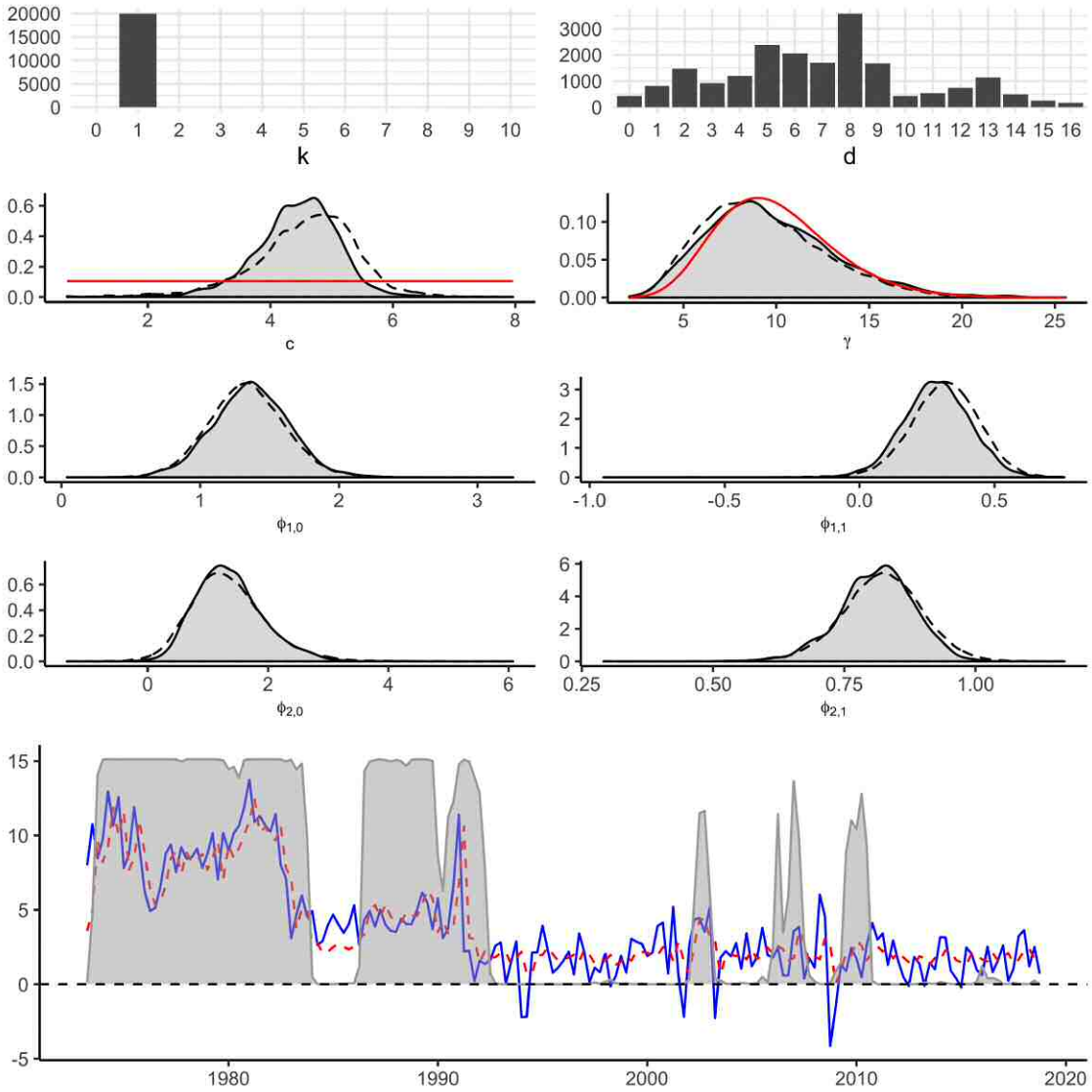

From top to bottom and left to right: (1) posterior draws for k, (2) posterior draws for d, (3)&(4) density of posterior draws for c and γ (black line and shaded area for density conditional on most commonly drawn k and d, black dashed line for unconditional density, red line prior density), (5)-(8) density of posterior draws for AR parameters $\boldsymbol{\phi}$ (black line and shaded area for density conditional on most commonly drawn k and d, black dashed line for density unconditional on d), (9) blue line inflation, dashed red line fitted inflation, dark grey line and shaded area rescaled implied transition function (conditional on most commonly drawn k and d). Computed from 20000 after burn-in draws for each model.

Appendix D Robustness analysis

D.1 Robustness for QoQ specification: SV errors

Table A1: Posterior estimates, all countries, annualized quarterly rate of change (QoQ), constant error variance.

	Quarterly rates of change								
	US			UK			Canada		
Parameter	$\theta_{0.5}$	$\theta_{0.025}$	$\theta_{0.975}$	$\theta_{0.5}$	$\theta_{0.025}$	$\theta_{0.975}$	$\theta_{0.5}$	$\theta_{0.025}$	$\theta_{0.975}$
$\phi_{1,0}$	1.40	0.76	2.10	-0.04	-0.65	0.63	1.24	0.65	1.94
$\phi_{1,1}$	0.49	0.27	0.73	1.03	0.88	1.18	0.36	0.02	0.63
$\phi_{2,0}$	1.07	-0.17	2.19	6.15	2.74	10.51	1.77	0.56	3.51
$\phi_{2,1}$	0.84	0.70	1.08	0.42	-0.01	0.71	0.76	0.57	0.91
k	1	(100%)	–	1	(100%)	–	1	(100%)	–
d	7	(8.45%)	–	0	(7.58%)	–	8	(7.23%)	–
γ	9.16	4.00	17.79	9.48	4.11	18.42	8.72	3.59	18.41
c	4.13	1.44	8.31	10.32	6.62	14.32	4.82	2.41	6.46
σ_c^2	3.63	3.00	4.53	5.78	4.58	7.30	3.64	2.92	4.49
δ^2	13.67	5.74	45.43	13.36	5.74	43.69	13.92	5.94	47.79
Λ	0.19	0.07	0.83	0.19	0.07	0.85	0.19	0.07	0.74

Median, 2.5%- and 97.5%-percentile of after burn-in parameter draws, conditional on the most commonly selected k and d as reported (share of total draws in parentheses). Computed from 20000 after burn-in draws for each model.

D.2 Heatmaps for QoQ specification

Figure D.2: Heatmap of transition function values F_t based on alternative filtering techniques, annualized quarterly rate of change.

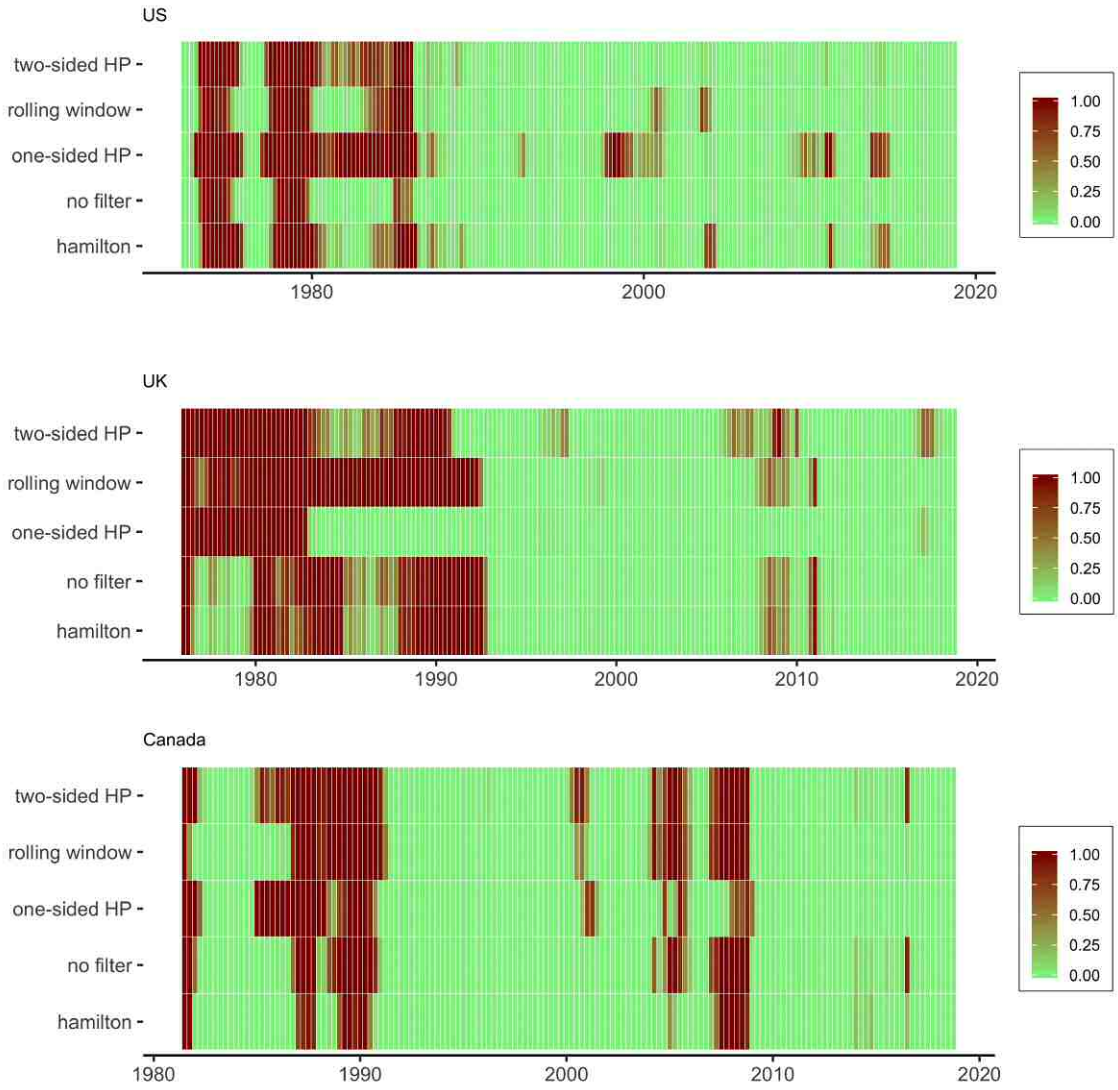

Each cell corresponds to one quarter. Color transitions from $F_t = 0$ (lightgreen) to $F_t = 1$ (darkred). F_t computed from median values, conditional on most commonly selected k and d for each model. Plots corresponding to: US, UK, Canada (from top to bottom). Computed from 20000 after burn-in draws for each model.

Figure D.3: Heatmap of transition function values based on different MA(q) orders, annualized quarterly rate of change.

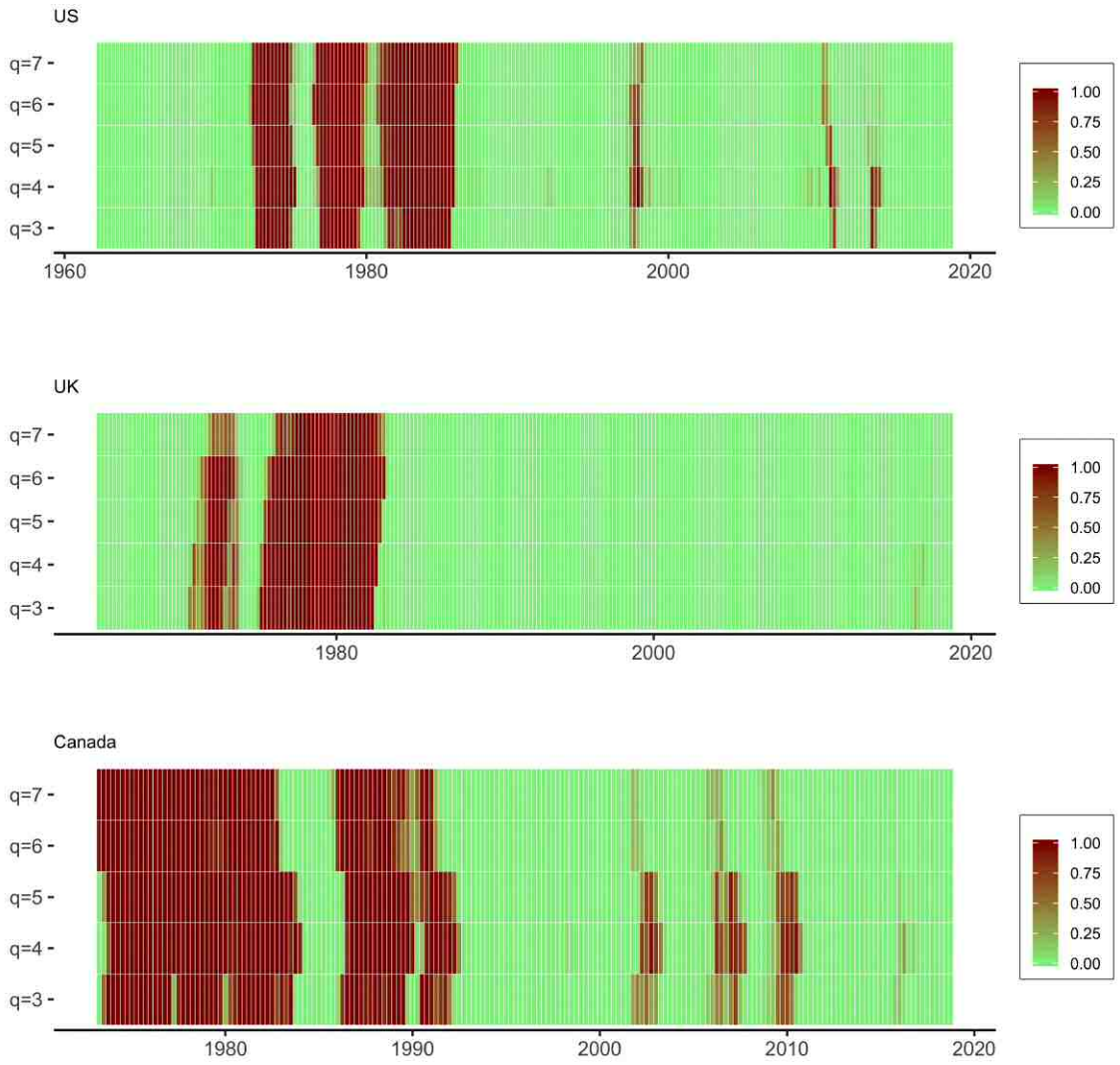

Each cell corresponds to one quarter. Color transitions from $F_t = 0$ (lightgreen) to $F_t = 1$ (darkred). F_t computed from median values, conditional on most commonly selected k and d for each model. Plots corresponding to: US, UK, Canada (from top to bottom). Computed from 20000 after burn-in draws for each model.

D.3 Robustness with respect to the implicit parameters specification

Figure D.4: Posterior histograms for delay parameter d based on alternative filtering techniques.

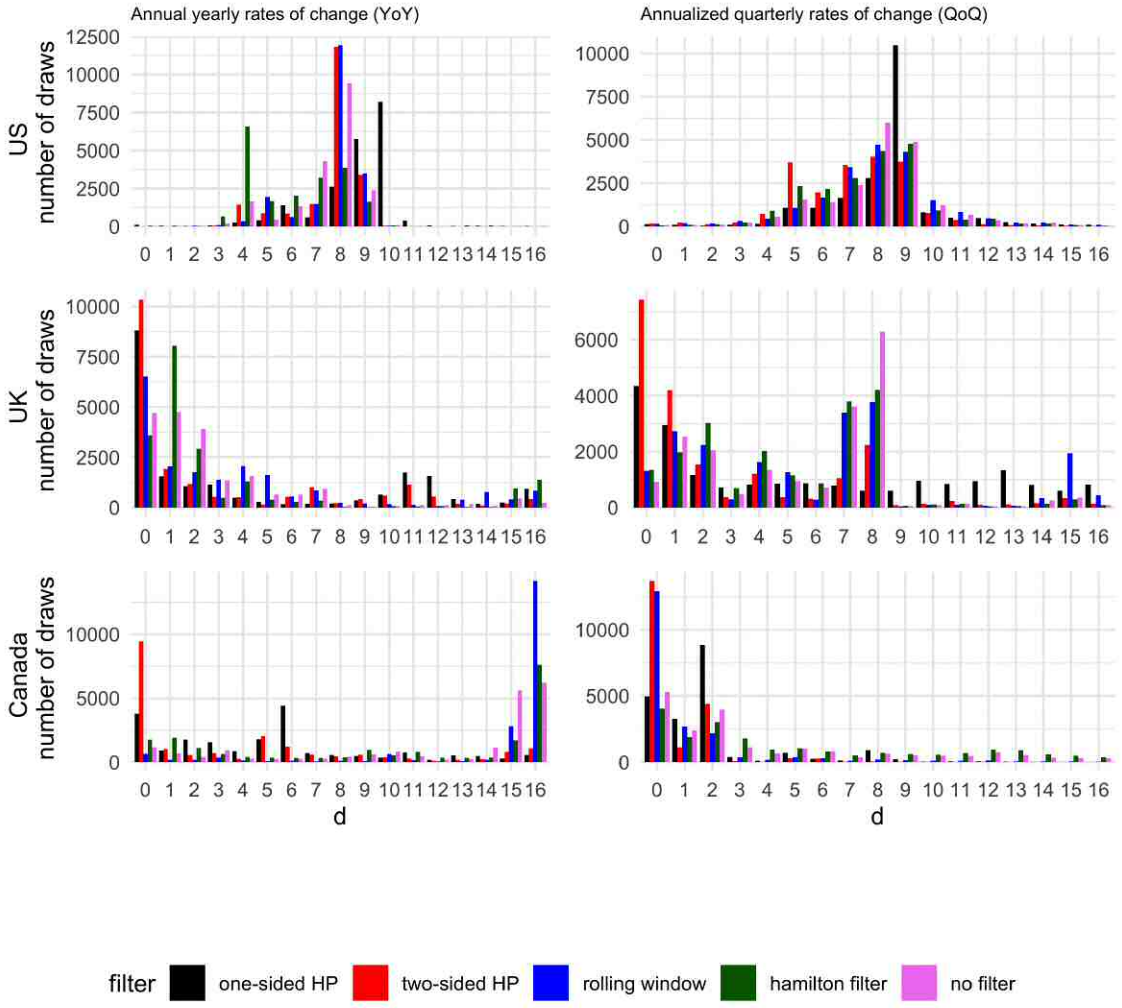

Histograms of posterior draws for the US (top panels), for the UK (middle panels), and for Canada (bottom panels). Results based on annual (YoY) rates of change (left hand side panels) and on annualized (QoQ) rates of change (right hand side panels). Computed from 20000 after burn-in draws for each model.

Figure D.5: Posterior density estimates for threshold parameter c based on alternative filtering techniques.

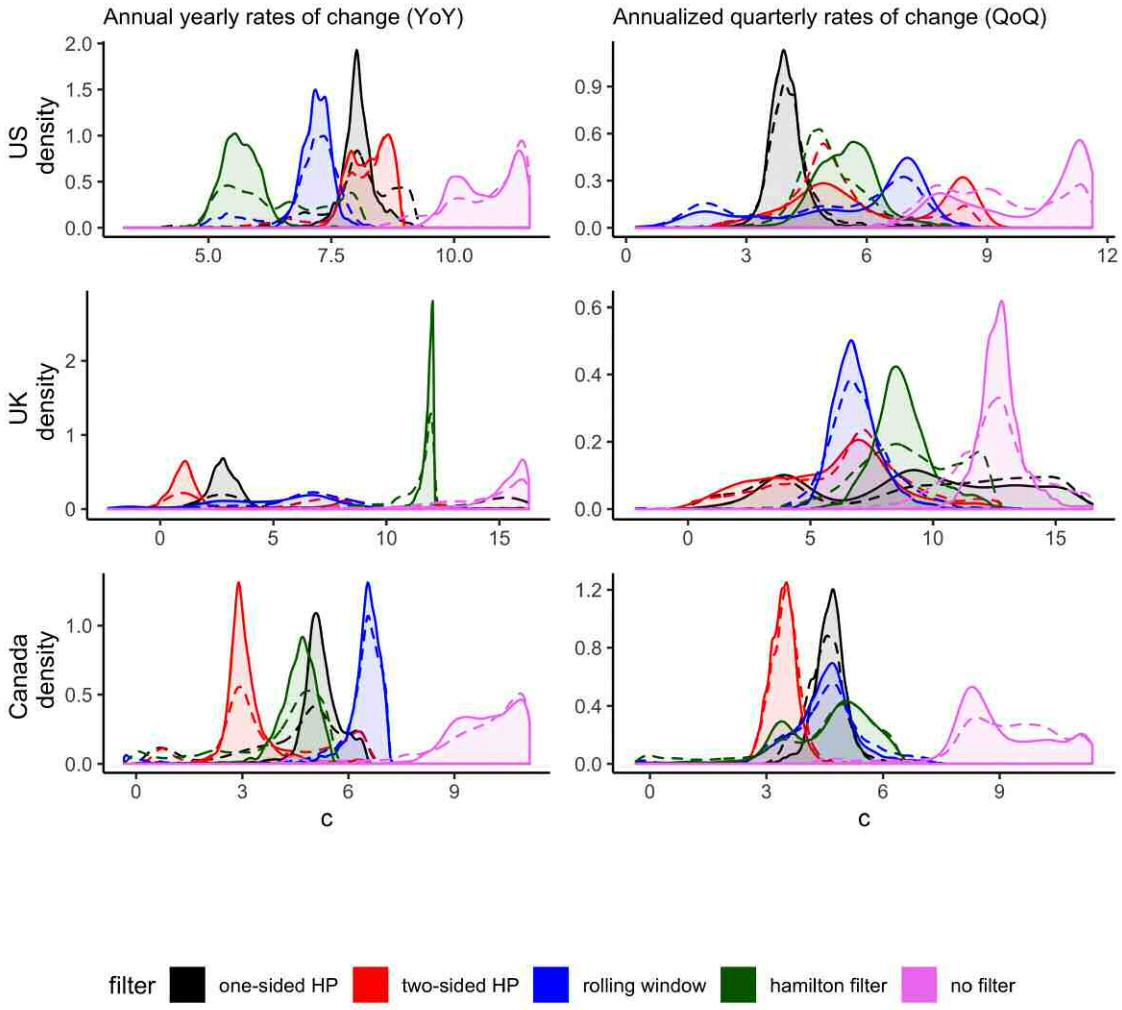

Density of posterior draws for the US (top panels), for the UK (middle panels), and for Canada (bottom panels). Results based on annual (YoY) rates of change (left hand side panels) and on annualized (QoQ) rates of change (right hand side panels). Lines and shaded areas correspond to the density conditional on the most commonly selected d for each model, dashed lines correspond to the density of c unconditional on d for each model. Computed from 20000 after burn-in draws for each model.

D.4 Posterior estimates with alternative filtering techniques

Table A2: Posterior estimates, all countries, alternative filter techniques, annual rates of change (YoY).

	Annual rates of change														
	US														
	one-sided HP filter			two-sided HP filter			rolling window filter			hamilton filter			no filter		
Parameter	$\theta_{0.5}$	$\theta_{0.025}$	$\theta_{0.975}$	$\theta_{0.5}$	$\theta_{0.025}$	$\theta_{0.975}$	$\theta_{0.5}$	$\theta_{0.025}$	$\theta_{0.975}$	$\theta_{0.5}$	$\theta_{0.025}$	$\theta_{0.975}$	$\theta_{0.5}$	$\theta_{0.025}$	$\theta_{0.975}$
$\phi_{1,0}$	0.29	0.14	0.43	0.29	0.13	0.44	0.32	0.17	0.47	0.35	0.17	0.53	0.27	0.12	0.43
$\phi_{1,1}$	0.90	0.85	0.94	0.90	0.85	0.94	0.89	0.84	0.93	0.86	0.80	0.92	0.90	0.85	0.95
$\phi_{2,0}$	-0.62	-1.26	0.16	0.60	-0.83	2.28	-0.85	-1.58	-0.15	-0.29	-0.98	0.42	0.39	-1.02	3.83
$\phi_{2,1}$	1.15	1.06	1.24	1.03	0.84	1.19	1.19	1.10	1.30	1.13	1.03	1.24	1.05	0.69	1.21
k	1	(100%)		1	(99.98%)	–	1	(100%)	–	1	(99.98%)	–	1	(100%)	–
d	10	(40.97%)	–	8	(59.17%)	–	8	(59.70%)	–	4	(32.96%)	–	8	(47.14%)	–
γ	9.87	4.97	17.17	9.38	4.92	17.57	10.02	4.94	17.24	7.78	3.94	14.11	9.24	4.73	16.09
c	8.03	7.36	8.81	8.31	7.58	8.86	7.21	6.65	7.75	5.63	4.98	6.51	10.70	9.55	11.51
ι	-1.26	-1.99	-0.30	-1.37	-2.06	-0.63	-1.34	-2.03	-0.61	-1.32	-2.10	-0.55	-1.34	-2.04	-0.56
ρ	0.86	0.64	0.97	0.82	0.59	0.95	0.84	0.60	0.96	0.88	0.69	0.98	0.83	0.61	0.96
σ^2	0.59	0.32	0.99	0.67	0.36	1.08	0.58	0.33	0.97	0.46	0.25	0.78	0.63	0.34	1.05
δ^2	13.63	5.75	46.28	13.70	5.63	46.96	13.56	5.69	46.18	13.62	5.71	44.63	13.69	5.64	45.56
Λ	0.19	0.07	0.77	0.19	0.07	0.81	0.18	0.07	0.80	0.19	0.07	0.80	0.19	0.07	0.82
	UK														
	one-sided HP filter			two-sided HP filter			rolling window filter			hamilton filter			no filter		
Parameter	$\theta_{0.5}$	$\theta_{0.025}$	$\theta_{0.975}$	$\theta_{0.5}$	$\theta_{0.025}$	$\theta_{0.975}$	$\theta_{0.5}$	$\theta_{0.025}$	$\theta_{0.975}$	$\theta_{0.5}$	$\theta_{0.025}$	$\theta_{0.975}$	$\theta_{0.5}$	$\theta_{0.025}$	$\theta_{0.975}$
$\phi_{1,0}$	0.12	-0.02	0.26	0.12	-0.19	0.29	0.16	-0.01	0.30	0.16	0.07	0.25	0.15	0.05	0.27
$\phi_{1,1}$	0.88	0.81	0.97	0.88	0.78	0.99	0.89	0.81	0.96	0.91	0.87	0.94	0.91	0.85	0.95
$\phi_{2,0}$	0.26	0.05	0.79	0.29	0.14	1.76	0.33	0.03	1.00	0.84	-0.56	2.28	1.35	0.09	3.83
$\phi_{2,1}$	0.93	0.84	0.99	0.92	0.82	0.97	0.93	0.83	1.00	0.97	0.73	1.20	0.86	0.51	1.05
k	1	(71.45%)	–	1	(67.88%)	–	1	(59.38%)	–	1	(72.30%)	–	1	(52.84%)	–
d	0	(44.05%)	–	0	(51.67%)	–	0	(32.61%)	–	0	(40.31%)	–	0	(52.84%)	–
γ	9.98	5.43	17.46	9.41	3.79	17.36	8.18	3.73	15.38	10.08	4.84	17.92	8.29	3.92	15.84
c	2.83	1.49	13.79	1.21	0.07	8.94	5.59	-1.42	10.21	11.91	10.46	12.08	15.52	10.14	16.28
ι	-1.23	-4.57	2.91	-1.24	-3.92	2.58	-1.28	-4.71	2.34	-1.19	-5.91	2.61	-1.20	-3.76	3.54
ρ	0.98	0.93	1.00	0.98	0.93	1.00	0.98	0.93	1.00	0.98	0.94	1.00	0.98	0.94	1.00
σ^2	0.40	0.26	0.60	0.39	0.25	0.59	0.39	0.26	0.60	0.36	0.23	0.57	0.35	0.22	0.54
δ^2	13.62	5.58	46.24	13.71	5.66	46.00	13.46	5.83	45.31	13.62	5.63	46.63	13.78	5.75	42.77
Λ	0.19	0.07	0.83	0.19	0.07	0.86	0.19	0.07	0.80	0.19	0.07	0.81	0.19	0.07	0.83
	Canada														
	one-sided HP filter			two-sided HP filter			rolling window filter			hamilton filter			no filter		
Parameter	$\theta_{0.5}$	$\theta_{0.025}$	$\theta_{0.975}$	$\theta_{0.5}$	$\theta_{0.025}$	$\theta_{0.975}$	$\theta_{0.5}$	$\theta_{0.025}$	$\theta_{0.975}$	$\theta_{0.5}$	$\theta_{0.025}$	$\theta_{0.975}$	$\theta_{0.5}$	$\theta_{0.025}$	$\theta_{0.975}$
$\phi_{1,0}$	0.29	0.08	0.51	0.38	0.19	0.59	0.20	0.00	0.39	0.24	0.03	0.45	0.25	0.04	0.45
$\phi_{1,1}$	0.85	0.75	0.94	0.78	0.69	0.87	0.94	0.86	1.01	0.93	0.84	1.01	0.92	0.83	1.00
$\phi_{2,0}$	1.80	-0.05	3.51	0.26	-0.24	0.84	0.21	-0.35	0.89	-0.18	-0.86	0.34	-0.20	-1.31	0.37
$\phi_{2,1}$	0.61	0.24	1.05	0.94	0.82	1.07	0.59	0.13	0.92	0.93	0.72	1.16	0.95	0.70	1.36
k	1	(100%)	–	1	(100%)	–	1	(100%)	–	1	(99.99%)	–	1	(99.98%)	–
d	6	(22.07%)	–	0	(47.17%)	–	16	(70.84%)	–	16	(38.15%)	–	16	(30.98%)	–
γ	9.65	4.67	17.65	9.96	4.95	17.98	9.44	4.90	17.04	9.72	5.04	17.30	9.50	4.66	16.48
c	5.17	3.88	6.35	3.00	2.25	5.29	6.56	5.26	7.07	4.65	3.18	5.39	9.95	7.99	11.09
ι	-1.29	-1.81	-0.83	-1.30	-1.82	-0.78	-1.38	-2.04	-0.78	-1.29	-1.91	-0.79	-1.32	-1.99	-0.78
ρ	0.79	0.23	0.95	0.81	0.36	0.96	0.81	0.48	0.95	0.78	0.39	0.94	0.78	0.38	0.95
σ^2	0.40	0.17	0.70	0.37	0.17	0.66	0.49	0.26	0.85	0.47	0.20	0.86	0.50	0.24	0.86
δ^2	13.82	5.74	47.77	13.65	5.70	44.96	13.53	5.72	45.84	13.54	5.68	45.51	13.68	5.72	43.62
Λ	0.19	0.07	0.86	0.19	0.07	0.81	0.19	0.07	0.82	0.19	0.07	0.81	0.19	0.07	0.77

Median, 2.5%- and 97.5%-percentile of after burn-in parameter draws, conditional on the most commonly selected k and d as reported (share of total draws in parentheses). Computed from 20000 after burn-in draws for each model. Source: own results.

Table A3: Posterior estimates, all countries, different MA(q) orders, annual rates of change (YoY).

Annual rates of change															
	US														
	q=3			q=4			q=5			q=6			q=7		
Parameter	$\theta_{0.5}$	$\theta_{0.025}$	$\theta_{0.975}$	$\theta_{0.5}$	$\theta_{0.025}$	$\theta_{0.975}$	$\theta_{0.5}$	$\theta_{0.025}$	$\theta_{0.975}$	$\theta_{0.5}$	$\theta_{0.025}$	$\theta_{0.975}$	$\theta_{0.5}$	$\theta_{0.025}$	$\theta_{0.975}$
$\phi_{1,0}$	0.25	0.13	0.38	0.25	0.12	0.39	0.26	0.14	0.40	0.27	0.13	0.40	0.26	0.13	0.40
$\phi_{1,1}$	0.91	0.88	0.95	0.91	0.87	0.95	0.91	0.87	0.95	0.91	0.87	0.95	0.91	0.87	0.95
$\phi_{2,0}$	-0.74	-1.75	0.18	-0.66	-1.50	0.16	-0.58	-1.25	0.21	-0.59	-1.17	0.20	-0.52	-1.09	0.25
$\phi_{2,1}$	1.17	1.07	1.31	1.16	1.06	1.29	1.15	1.05	1.24	1.15	1.05	1.23	1.14	1.05	1.21
k	1	(99.90%)	–	1	(100%)	–	1	(100%)	–	1	(99.99%)	–	1	(99.90%)	–
d	11	(43.91%)	–	10	(58.58%)	–	10	(38.48%)	–	9	(42.74%)	–	9	(26.85%)	–
γ	9.53	5.00	16.27	8.83	4.37	16.07	9.70	4.91	17.12	9.42	4.76	16.28	10.29	5.52	18.22
c	8.55	7.92	9.13	8.05	7.28	9.12	8.04	7.35	8.76	7.56	6.96	8.84	7.68	7.04	8.37
δ^2	13.66	5.76	47.50	13.62	5.77	45.66	13.64	5.61	45.88	13.65	5.75	46.31	13.62	5.58	43.08
Λ	0.18	0.07	0.80	0.19	0.07	0.82	0.18	0.07	0.83	0.19	0.07	0.84	0.19	0.07	0.81
ι	-1.45	-2.10	-0.82	-1.45	-2.13	-0.81	-1.44	-2.13	-0.81	-1.45	-2.13	-0.81	-1.43	-2.05	-0.79
ρ	0.86	0.66	0.96	0.85	0.66	0.96	0.86	0.67	0.96	0.86	0.66	0.96	0.86	0.65	0.96
σ^2	0.54	0.30	0.90	0.55	0.30	0.89	0.55	0.32	0.87	0.56	0.32	0.91	0.55	0.33	0.92
	UK														
	q=3			q=4			q=5			q=6			q=7		
Parameter	$\theta_{0.5}$	$\theta_{0.025}$	$\theta_{0.975}$	$\theta_{0.5}$	$\theta_{0.025}$	$\theta_{0.975}$	$\theta_{0.5}$	$\theta_{0.025}$	$\theta_{0.975}$	$\theta_{0.5}$	$\theta_{0.025}$	$\theta_{0.975}$	$\theta_{0.5}$	$\theta_{0.025}$	$\theta_{0.975}$
$\phi_{1,0}$	0.07	0.00	0.15	0.07	0.00	0.16	0.08	0.00	0.16	0.06	-0.03	0.14	0.05	-0.03	0.13
$\phi_{1,1}$	1.57	1.35	1.70	1.56	1.31	1.70	1.56	1.40	1.69	1.58	1.44	1.72	1.57	1.43	1.72
$\phi_{1,2}$	-0.61	-0.73	-0.41	-0.60	-0.73	-0.39	-0.60	-0.73	-0.44	-0.60	-0.74	-0.46	-0.60	-0.74	-0.46
$\phi_{2,0}$	2.57	0.04	6.56	2.27	-0.06	5.94	2.36	-0.35	6.45	0.78	-0.03	2.68	1.13	0.07	3.14
$\phi_{2,1}$	0.83	-0.02	1.64	1.00	0.07	1.64	0.92	0.00	1.63	1.30	0.84	1.72	1.29	0.81	1.73
$\phi_{2,2}$	-0.15	-0.76	0.54	-0.27	-0.76	0.46	-0.20	-0.78	0.52	-0.47	-0.96	-0.08	-0.52	-1.01	-0.11
k	2	(99.83%)	–	2	(99.76%)	–	2	(99.77%)	–	2	(98.80%)	–	2	(99.83%)	–
d	0	(55.10%)	–	0	(40.19%)	–	0	(28.18%)	–	16	(19.50%)	–	16	(29.59%)	–
γ	9.29	4.37	17.34	9.23	4.35	16.79	9.41	4.68	16.84	9.13	3.96	16.55	9.10	4.34	16.24
c	14.87	3.50	15.82	14.35	3.31	15.45	14.54	5.79	15.44	12.98	6.23	15.51	14.39	6.67	15.37
δ^2	10.74	4.88	30.69	10.68	4.85	30.99	10.71	4.94	30.69	10.78	4.86	31.44	10.55	4.91	29.64
Λ	0.14	0.06	0.45	0.14	0.06	0.47	0.14	0.06	0.48	0.14	0.06	0.47	0.14	0.06	0.47
ι	-1.91	-4.40	0.26	-1.87	-4.46	0.27	-1.84	-4.50	0.40	-1.90	-4.74	0.52	-1.97	-4.62	0.78
ρ	0.97	0.92	1.00	0.97	0.93	1.00	0.97	0.93	1.00	0.97	0.92	1.00	0.97	0.92	1.00
σ^2	0.35	0.22	0.53	0.34	0.22	0.52	0.35	0.22	0.54	0.36	0.24	0.54	0.38	0.24	0.61
	Canada														
	q=3			q=4			q=5			q=6			q=7		
Parameter	$\theta_{0.5}$	$\theta_{0.025}$	$\theta_{0.975}$	$\theta_{0.5}$	$\theta_{0.025}$	$\theta_{0.975}$	$\theta_{0.5}$	$\theta_{0.025}$	$\theta_{0.975}$	$\theta_{0.5}$	$\theta_{0.025}$	$\theta_{0.975}$	$\theta_{0.5}$	$\theta_{0.025}$	$\theta_{0.975}$
$\phi_{1,0}$	0.63	0.27	1.24	0.67	0.29	1.35	0.52	0.23	1.30	0.42	0.17	1.20	0.36	0.17	0.62
$\phi_{1,1}$	0.67	0.39	0.83	0.66	0.34	0.82	0.71	0.30	0.84	0.76	0.31	0.87	0.79	0.66	0.87
$\phi_{2,0}$	-0.04	-0.25	0.24	-0.06	-0.29	0.25	0.01	-0.23	0.30	0.05	-0.21	0.41	0.11	-0.18	0.47
$\phi_{2,1}$	1.01	0.97	1.05	1.01	0.97	1.06	1.01	0.96	1.05	1.01	0.96	1.05	1.00	0.95	1.04
k	1	(100%)	–	1	(100%)	–	1	(100%)	–	1	(99.99%)	–	1	(100%)	–
d	2	(82.03%)	–	2	(71.23%)	–	1	(75.93%)	–	0	(45.59%)	–	0	(45.55%)	–
γ	6.89	2.98	13.62	7.20	2.90	14.11	6.80	2.96	14.28	6.53	2.75	14.10	8.49	3.86	15.75
c	1.85	0.73	4.23	2.06	0.88	4.21	2.49	0.87	4.28	2.84	0.80	5.32	3.59	2.53	5.17
δ^2	13.61	5.71	46.21	13.59	5.66	45.72	13.64	5.63	46.08	13.62	5.58	44.88	13.51	5.58	47.16
Λ	0.19	0.07	0.83	0.19	0.07	0.82	0.19	0.07	0.81	0.19	0.07	0.78	0.19	0.07	0.80
ι	-1.22	-1.75	-0.70	-1.20	-1.74	-0.67	-1.21	-1.72	-0.73	-1.21	-1.71	-0.70	-1.21	-1.70	-0.66
ρ	0.86	0.60	0.97	0.86	0.61	0.97	0.85	0.56	0.96	0.85	0.57	0.96	0.85	0.61	0.96
σ^2	0.35	0.18	0.58	0.33	0.16	0.57	0.34	0.18	0.56	0.36	0.19	0.59	0.36	0.19	0.59

Median, 2.5%- and 97.5%-percentile of after burn-in parameter draws, conditional on the most commonly selected k and d as reported (share of total draws in parentheses). Computed from 20000 after burn-in draws for each model. Source: own results.

Figure D.1: Time-varying versus constant error variance, all countries, annualized quarterly rates of change.

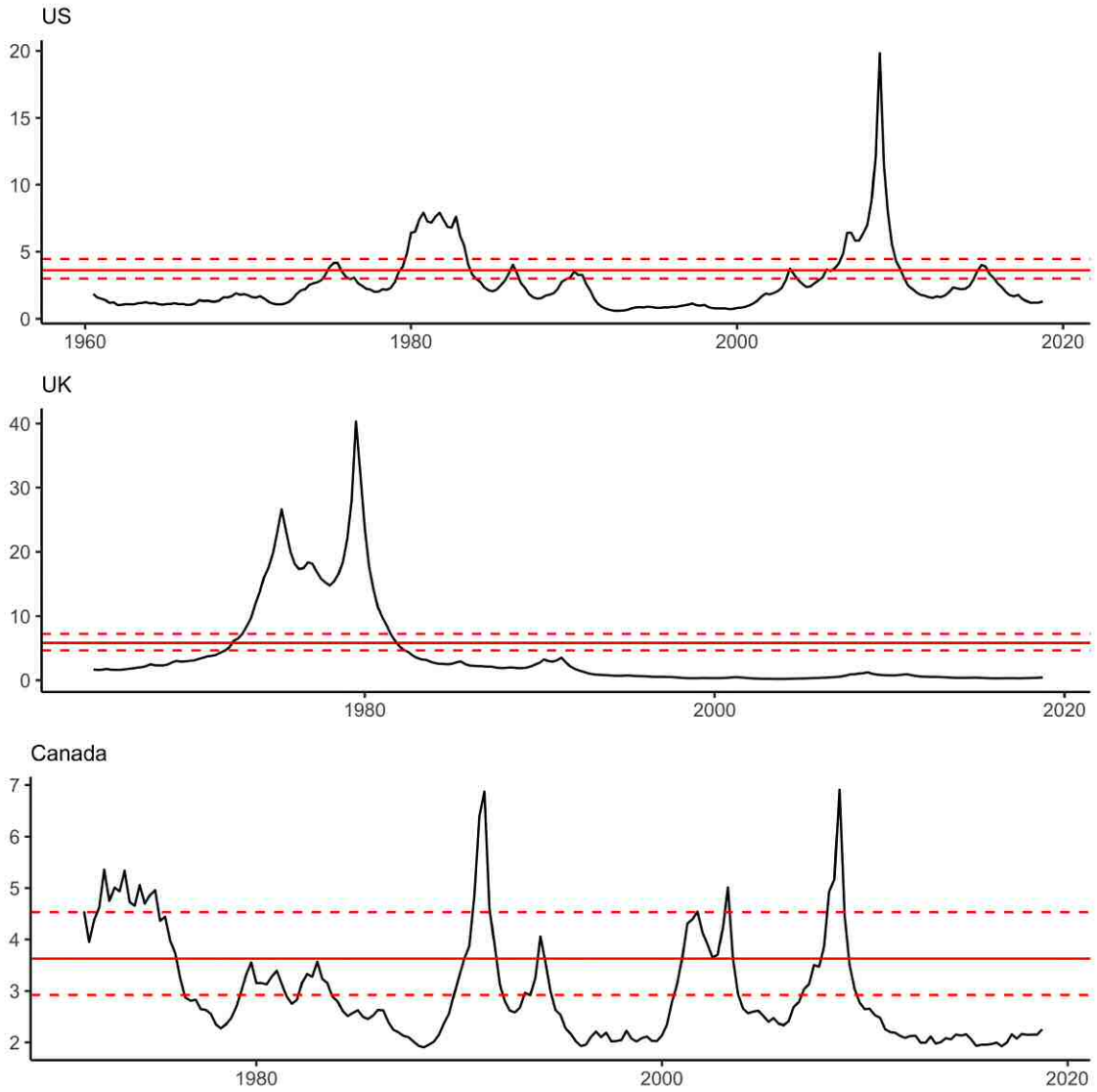

Median of posterior draws for time-varying variance, i.e. $exp(\boldsymbol{h})$, (black line), horizontal lines imply median (red line) and 95% confidence set (red dashed line) values of posterior draws for constant error variance σ_c^2. Plots corresponding to: US, UK, Canada (from top to bottom). Computed from 20000 after burn-in draws for each model.